NAIST-IS-DD1161206

Doctoral Dissertation

Studies on Signal Processing for Local Ocean Wave Monitoring System

Maricris Cuison Marimon

September 17, 2014

Department of Information Science
Graduate School of Information Science
Nara Institute of Science and Technology

A Doctoral Dissertation
submitted to Graduate School of Information Science,
Nara Institute of Science and Technology
in partial fulfillment of the requirements for the degree of
Doctor of ENGINEERING

Maricris Cuison Marimon

Thesis Committee:

Professor Kenji Sugimoto	(Supervisor)
Professor Minoru Okada	(Co-supervisor)
Visiting Professor Kentaro Hirata	(Co-supervisor)
Assistant Professor Takamitsu Matsubara	(Co-supervisor)

Studies on Signal Processing for Local Ocean Wave Monitoring System*

Maricris Cuison Marimon

Abstract

Ocean Wave Monitoring is an essential activity that provides valuable data used for travel statuses of maritime transportations, for modeling offshore infrastructures and for producing wave forecasts. There are various ocean wave monitoring systems that are utilized nowadays ranging from in-situ to remote or a combination of both. The complexity of the mechanism and technology utilized by the wave monitoring system defines its construction and operation cost. This study utilized and operated a low cost local wave monitoring system that is reliable and robust. This system is an alternative to sophisticated wave monitoring systems. This consists of wave sensors that are relatively cheap and ubiquitous such as MEMS-enabled devices. These devices are popular to the sensing community because they are easy to build, program and use, and they can be utilized in any application and environment. These devices are advantageous because they can be connected to a network that can be smartly expanded to monitor the area of interest.

This study aims to explore on processing techniques that enables the local wave monitoring system to (1) detect severe wave conditions (2) process data from its multiple sensors and (3) properly classify wave conditions. By having these functions, the system will have similar abilities to sophisticated wave monitoring systems but with relatively much lower construction and operation costs. Since the system considered for this is an alternative system, there is one major challenge encountered. The wave sensors in the system have certain limitations

*Doctoral Dissertation, Department of Information Science, Graduate School of Information Science, Nara Institute of Science and Technology, NAIST-IS-DD1161206, September 17, 2014.

in processing power, memory and battery power of the devices hence, the data collected are short length time series data. Typically in conventional methods, they require longer time series data for generating significant wave height and period hence, these methods cannot be utilized in the alternative system. Due to this, the processing techniques should be able to address this issue. Also, if this issue is properly addressed, the alternative system will have an advantage to the conventional systems because acquiring and processing short time series data can be done quickly hence immediate publication of wave information is possible.

For the detection of severe wave conditions, two signal processing techniques are explored. First technique is the thresholding technique that processes instantaneous data gathered by the sensors. This technique enables the sensors to judge the condition of its area and preprocess the data before sending relevant information to the central receiver of the network. This aims to compress the data that is relayed to the network. This is rather a straight-forward and stringent approach because the threshold levels are fixed. It is important to note that wave conditions in different areas can vary depending on the bathymetry of the location even if they are experiencing the same conditions. The threshold level set in one location might not be enough for the other location. Because of this, the second technique is explored. The second technique uses higher order statistics to evaluate data segments gathered by sensors. The sensors are allowed to gather data first on the specific location on a relatively calm day to have a base data and then, the statistical parameters are generated. These values are location specific and are the bases of comparison for each of the wave segment gathered by the sensors. Higher differences from the base data indicate that the wave conditions are more severe.

For the processing of the multiple sensors in the monitoring system, this study explored Independent Component Analysis (ICA). This technique is utilized in separating source signals from multiple sensors in a network or in an area. This is useful in getting or estimating dominant patterns of source signals in a very noisy environment which are typically experienced in field experiments or in real data. Though of its potential, this technique falls short to the aim of the study. Wave data has certain characteristics that does not meet the requirements for a good implementation of independent component analysis.

For the classification of wave conditions, this is done through employing Support Vector Machines (SVM). This technique initially uses spectral analysis technique which decomposes the wave data into frequencies. The significant wave height and wave period are then calculated from the wave spectra. These two values are the features considered for the SVM. The SVM trains the data to create a classification model for ocean wave conditions. By having the classification model, identification of wave conditions can be done immediately hence information can be readily published.

All of the processing techniques used the short time series data and were able to assess the data. These techniques were able to provide information immediately hence immediate publication of wave condition is possible.

Keywords:

Ocean Wave Monitoring, Low Cost Wave Sensors, Signal Processing, Sensor Network, Statistical Analysis, Machine Learning, Support Vector Machine

Contents

List of Figures

List of Tables

List of Symbols

ζ	elevation of the water surface relative to the mean water level
H	wave height
H_{rms}	root mean square height
H_s or $H_{\frac{1}{3}}$	significant wave height
$\overline{H}$	mean wave height
$H_{r_{\frac{1}{3}}}$	significant wave height derived from Rayleigh Distribution
$S(\omega)$	wave spectrum
m_0	zero-th moment of the spectrum
U_w	wind speed at $19.5m$ above mean sea level
g	$9.8m/s^2$
T	wave period
T_0	mean zero crossing period
T_m	mean wave period
T_s	significant wave period
C	penalty parameter
γ	Radial Basis Kernel Hyperparameter

Chapter 1

Introduction

This chapter introduces the theme of the dissertation: Section 1.1 presents the significance of building an effective local ocean wave monitoring system which can provide valuable data that can be used in modeling offshore structures, safe marine transportation and wave forecasts. Section 1.2 explains the current problems of wave monitoring and the challenges of finding an effective signal processing technique that will address these problems. Section 1.3 to 1.4 present the contribution and merits of the signal processing techniques utilized in the study. Lastly, Section 1.5 gives the outline for the chapters of this dissertation paper.

1.1 Research Motivation

Ocean wave monitoring is a thorough assessment activity on ocean surfaces. This activity is done by researchers and organizations who are interested in the dynamics of the ocean waves. The data collected in this activity are significant for constructing robust offshore marine structures. They are also used in characterizing a location's potential for wave energy farms which can be an alternative source of energy. Also, the data is directly important in producing wave alarm systems for sea farers. There are several wave monitoring systems that utilize different techniques ranging from simple to complicated. These techniques vary depending on the purpose and coverage area of the wave monitoring system. In-situ wave monitoring targets a more detailed point measurement type of data while remote wave monitoring aims for a wider coverage type of data. Most current wave

monitoring system are expensive to build because they usually utilize sophisticated and dedicated devices as sensors. Construction and operational costs sky rocket as the wave monitoring system is utilized. These systems are not easily assembled and sometimes, they are not so user friendly since the operators need certain trainings to operate it. Because of the expensive undertaking, building them for independent and small scale research might not be practical. Also, they are expensive for massive deployments in third world countries. This work is a continuing activity of [5] which is largely motivated with the necessity of wave alarm systems in the Philippines.

The Philippines is an archipelago located in an area surrounded by big bodies of water namely the Pacific Ocean and the South China Sea. Because of this geographical characteristic, a large percent of its population live in coastal areas hence the primary source of living and economy greatly relies on seas. Also, because of its location, it is bombarded with harsh monsoon systems that causes violent seas. With a rate of 20 typhoons per year, sea related activities are of constant threat. The two most vulnerable industries are the transportation and tourism industries. Watercraft ranging from small boats, barges to ships that are mainly used to transport people and products are prone to accidents when there are typhoons or unexpected rouge waves. Figure 1.1 shows the recorded maritime accidents from year 1995 to 2006. Due to the fact that tourism in the Philippines rely on island hopping activities, the safety of the tourists is always at stake because of the lack of warning systems.

There is an existing wave monitoring system in the Philippines but it is currently tied with a government agency. They have a buoy that is capable of measuring barometric pressure, wind speed and direction, air and sea surface temperature and wave height. Though of its sophistication, it is not sufficient to gather data that is representative of the whole Philippines. Also, since this is under a government agency, data access is limited for researchers.

Clearly, there is a call to build alternative wave monitoring systems that can provide information to the public. These monitoring systems do not have to be expensive since these systems can utilize readily available MEMS-based sensors that are easy to construct and use. The motivation of this study is to explore signal processing techniques that can be used in these sensors that will make

All VESSEL TYPE	1995	1996	1997	1998	1999	2000	2001	2002	2003*	2004	2005	2006
Aground	58	19	5	42	44	21	27	22	35	48	19	21
Sunk	37	35	16	37	37	25	21	23	35	24	17	23
Collision	17	5	6	5	5	14	11	10	20	11	5	1
Caught Fire	23	6	8	9	11	7	10	15	12	7	7	8
Capsized	33	32	11	88	109	47	49	44	67	64	34	25
Missing	0	0	0	12	0	1	5	6	24	11	4	18
Drifted/Engine Trouble	13	9	9	8	0	14	17	20	37	39	12	17
Flooding	0	3	0	0	0	2	1	1	2	4	4	0
Rammed	0	10	2	6	0	3	6	5	15	5	4	1
Others	0	0	1	1	57	17	21	6	10	13	16	0
SUMMARY												
Number of Incident	181	119	58	208	263	151	168	152	245	226	122	114
Number of SAR Mission	57	57	34	86	219	50	88	65	53	84	108	53
Number of Casualties	121	82	48	161	223	177	5	73	74	144	25	62
Number of Person Missing	97	38	20	174	127	102	74	146	232	116	47	94
Person Rescued/Survivors	2,050	1,424	347	1,339	3,828	2,771	1,969	1,178	2,903	4,893	2,920	5,121

Source: Philippine Coast Guard (PCG)
Note: * The source for 2003 data is the Maritime Industry in the Philippines Databook 2005

Figure 1.1: Summary of Maritime Accidents in the Philippines from 1999 to 2006

the system effective and accurate. This is interesting because wave monitoring processes are complex to do and conventional methods have certain requirements that aren't necessarily met by the considered devices.

1.2 Overview of the problem

This study aims to enable the alternative local ocean wave monitoring system (1) detect severe wave conditions, (2) process data from its multiple sensors and (3) properly classify wave conditions. These functions make the local wave monitoring system similar to sophisticated and expensive monitoring systems. Enabling the alternative system to do these functions needs a good consideration of the kind of data that the system gathers. Since the system's sensors are deployed on seas, the sensors are configured to save battery and memory hence the data acquisition duration is kept short producing short time series wave data.

These short time series wave data has both advantages and disadvantages. Other than promoting the system's battery and memory conservation as an advantage, this kind of data allows the system to publish immediate wave information. This is because the system only takes a short duration to collect and process such data assuming that the system utilizes a good processing technique.

The major disadvantage of these short time series wave data is that most algorithms used in conventional systems cannot be utilized to process these data. Note that conventional wave monitoring systems have enough battery and memory capacity to gather long time series data. Naturally, the methods conceptualized and utilized in these systems address and use long time series data. Also, short time series data are very dynamic and prone to noise. They are also not stationary data. Conventional methods such as Fast Fourier Transform (FFT) considers stationary data. There is significant information loss if FFT is utilized in short time series data. Therefore, the processing techniques considered for this short time series data should have a different mechanism as compared to the conventional methods.

1.3 Research contribution

The main contribution of this dissertation is to enable an alternative local ocean wave monitoring system to (1) detect severe wave conditions, (2) to process data from its multiple sensors and (3) to properly classify wave conditions using techniques that process short time series data. This promotes the system to be an equal counterpart of sophisticated systems but at a lower cost. For the detection of severe wave conditions, thresholding technique and statistical analysis technique are explored. For the processing of data from multiple sensors, independent component analysis is explored. For the classification of wave conditions, support vector machine is used to generate a classification model of wave conditions.

1.4 Research tasks and limitations

This study has two sets of main activities in gathering data for the techniques. First set of activities is the field experiments. The local ocean wave monitoring

system was deployed on five different locations in the Philippines as shown in Figure 1.2. One location is located in Manila Bay and the other four are located in Davao Gulf. The locations are chosen because they have unique coastal characteristics. The first one is on Manila Bay which is a sheltered bay. Second location is in the strait between Davao City and Island Garden City of Samal (IGACOS). This location is deep enough for ships to navigate to a nearby pier. Third location is on the coast of Davao which is in close proximity of a nearby island, IGACOS. Fourth location is on the coast of IGACOS which is opposite to the third location. The fifth location is on the coast of Davao which is far from IGACOS. This location has access to open seas. It is noted that most part of Davao Coast is obstructed from open sea due to IGACOS. Also, in order to keep the other factors from affecting the experiments, the deployment weather conditions were relatively fair.

The second set is the computer simulations. One simulation is done through Matlab which generates various m-sequence or pseudorandom binary data. These data are utilized in testing ICA. Other simulation is for generating wave data. This is done through a program that uses the JONSWAP wave spectra model. Different wave conditions are generated through this program. This simulation offers a quick way to have labelled data needed for Support Vector Machines. Despite that the wave data is to be generated through a spectra model, the input variables in the model are taken with the consideration of the statistical characteristics from the long term data [4]. This treatment makes the data more realistic than theoretical.

The limitation of this study is that it does not modify the hardware of the sensors in the local wave monitoring considered. The processing techniques use the short time series data as produced in the local wave monitoring system.

1.5 Dissertation layout

The dissertation is presented and organized as follows:

This chapter introduced the importance of ocean wave monitoring systems for research, modeling offshore structures and construction of wave alarm systems. It also presented the challenges encountered in wave monitoring systems

(a) Philippine Map

(b) Davao City Map

Figure 1.2: Deployment Locations of the Local In-situ Ocean Wave Monitoring System

and the motivation of this study. It also described the research contributions, tasks, limitations and the dissertation layout. **Chapter Two** gives the related literature and works. In order to have a thorough understanding of the mechanics and purpose of the wave monitoring system, the theoretical concepts of waves and the descriptions of wave conditions are discussed. The conventional processing techniques are also discussed. Since there are several existing ocean wave monitoring systems, the types of monitoring systems are thoroughly expanded in this chapter. **Chapter Three** presents the overview of the local wave monitoring system considered in this study. It also discusses the individual components and the features of the system. It also expounds the system processes. **Chapter Four** gives the detailed exploration and testing of techniques for the detection of severe wave conditions. It discusses the concepts of the Threshold technique and the Statistical Analysis technique. It also shows the results of these explorations and testing. **Chapter Five** presents the details of the processing of multiple sensors through the Independent Component Analysis technique. It will discuss the experimental setups for the simulations and the experiment results. **Chapter Six** presents the details on the classification of ocean wave conditions. This section presents the conventional method utilized in sophisticated systems. It shows the mechanism, advantage and disadvantages to this method. Since the conventional method does not suffice the needs of the local ocean wave monitoring system, this section presents the proposed method which uses Support Vector Machine to classify wave conditions. It gives a thorough discussion on the preprocessing steps done for the data, kernel setups for SVM and the considerations. It also shows and discusses the results of the experiments. **Chapter Seven** provides the conclusion of this study. **Chapter Eight** presents the recommendations and the future works of this study.

Chapter 2

Related Works

2.1 Theoretical Concepts of Waves

In order to properly establish an ocean wave monitoring system, it is important to understand the theoretical concepts of waves [6] [1]. Through the basic understanding of ocean waves and the forces that govern them, considerations can be made in the design of a robust ocean wave monitoring system [7].

A sinusoidal wave profile can be mathematically expressed as:

$$\zeta = a\cos(kx - \omega t) = \frac{H}{2}\cos(\frac{2\pi x}{L} - \frac{2\pi t}{T}) = a\cos\theta, \tag{2.1}$$

where ζ is the elevation of the water surface relative to the mean water level, a is the wave amplitude, $k = 2\pi/L$ is the wave number, $\omega = 2\pi/T$ is the angular or radian frequency, H is the wave height, T is the wave period and $\theta = kx - \omega t$. This expression describes a periodic, sinusoidal, progressive wave traveling in the positive x direction. For waves moving in negative x direction, the minus sign before the $\frac{2\pi t}{T}$ is replaced with a plus sign.

Equation (2.1) presents that a sinusoidal wave profile solves the linearized equations of motions. A real sea surface may be represented as the sum of a large number of simple sinusoids with independent amplitudes and phases [8]. This is shown in Figure 2.1. The time history of sea surface wave height viewed at fixed location are expressed as a combination of sinusoids:

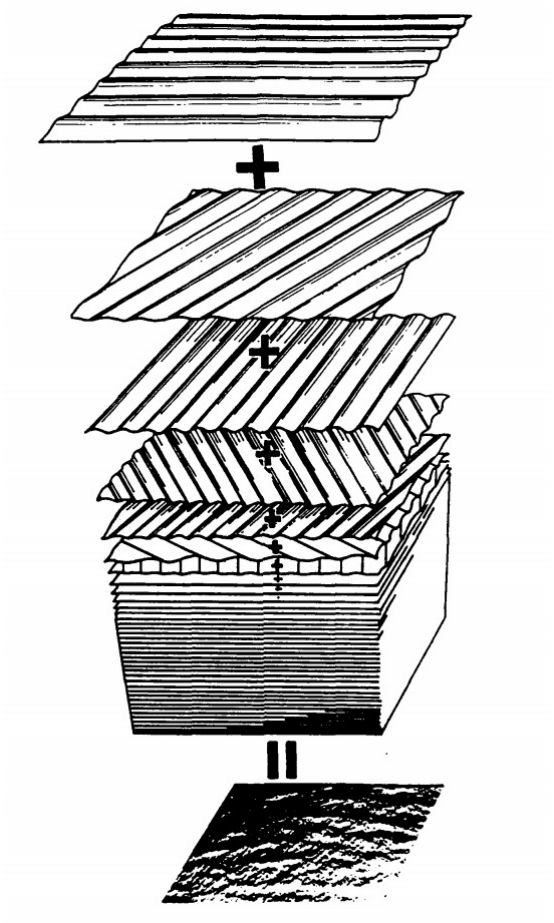

Figure 2.1: Superposition of long crested, sinusoidal wave trains that produces a random sea surface [1]

The sinusoidal wave profile can also be mathematically expressed as:

$$\zeta(t) = \sum_n a_n \sin(\omega_n t - \phi_n), \tag{2.2}$$

where the subscript n refers to the n^{th} component, ζ surface elevation about the mean sea level, ω_n is the angular frequency, and ϕ_n is the phase angle. Values of ζ are real independently distributed random variables with finite variances. Values of ϕ_n are independently and uniformly distributed in the interval $(0,\, 2\pi)$.

For actual wave records or data, wave-by-wave analysis can be done. It determines the wave properties by finding average statistical quantities of individual

wave components present in the wave record. Wave records are required to be long enough to contain several hundred waves for the calculated statistics to be reliable. This is a manual process of identifying the heights and periods of the individual wave components followed by simple counting of zero-crossings and wave crests in the wave record.

There are many short term parameters which are used in defining statistics of actual wave data. The most common ones are the characteristic wave height, H_c and the characteristic wave period, T_c.

Characteristic wave height can be defined in many ways. These include mean height, root-mean-square height and mean height of the highest one-third of all waves known as significant wave height, H_s or $H_{\frac{1}{3}}$. The characteristic wave period could also be defined as mean period or average zero-crossing period.

Significant wave height, H_s or $H_{\frac{1}{3}}$, is the most important wave parameter used in describing sea states. The most direct way of getting this parameter is to rank waves in a wave record and then choose the highest one-third of the waves. The average of this highest one-third of the waves is the significant wave height:

$$H_s = H_{\frac{1}{3}} = \frac{1}{\frac{N}{3}} \sum_{i=3}^{N/3} H_i, \tag{2.3}$$

where N is the number of individual wave heights H_i in a record ranked from highest to lowest.

The statistical properties of a random signal like the wave surface profile can be obtained from a set of many observations taken in different locations (i.e. multiple sensors in a network) which are called an ensemble. In order to determine wave properties from the process ζ, there are assumptions made with its time and spatial variations.

ζ should be stationary which means that its statistical properties are independent of the origin of the time measurement. It should be homogenous which means that its properties are invariant with the locations. It should also be ergodic. The statistics of any measured ζ is same as the average across the whole ensemble.

The mean or expected value of the sea state, μ_n or $E[\zeta]$ is defined as:

$$\mu_n = E[\zeta(t)] = \frac{1}{\tau} \int_{\frac{-\tau}{2}}^{\frac{\tau}{2}} \zeta(t) dt. \tag{2.4}$$

The variance of ζ is expressed as:

$$\sigma_n^2 = E[\zeta^2] - \mu_n^2. \tag{2.5}$$

The standard deviation σ_n is the square root of the variance and is also called as the second central moment of $\zeta(t)$. It shows the spread of the values of $\zeta(t)$ about its mean.

Actual waves are considered as random signals. It is very difficult to mathematically calculate hence some probability laws are followed so that wave statistics can be readily obtained analytically [9] [10]. [11] proposed to use statistical theory to the random water surface elevation of ocean waves to describe their statistics. There are two probability distributions that are used in the study of random ocean waves - Gaussian distribution and Rayleigh distribution.

Gaussian probability density is given by the equation:

$$p(x) = \frac{1}{\sigma_x \sqrt{2\pi}} \exp\left(-\frac{(x-\mu_x)^2}{2\sigma_x^2}\right), \tag{2.6}$$

where μ_x is the mean of x and σ_x is the standard deviation.

Rayleigh probability density is:

$$p(x) = \frac{\pi x}{2\mu_x^2} \exp\left[\frac{-\pi}{4}\left(\frac{x}{\mu_x}\right)^2\right], \tag{2.7}$$

for $x \geq 0$ where μ_x is the mean.

The heights of the individual waves can be regarded as a stochastic variable represented by a probability distribution. For the Rayleigh distribution, wave heights are:

$$p(x) = \frac{2H}{H_{rms}^2} \exp\left[\frac{-H^2}{H_{rms}^2}\right], \tag{2.8}$$

where:

$$H_{rms} = \sqrt{\frac{1}{N}\sum_{j=1}^{N} H_j^2}. \tag{2.9}$$

The significant height $H_{r_{\frac{1}{3}}}$ from Rayleigh distribution is the centroid of the area for $H \geq H_*$ under the density function where $H > H_*$ corresponds to waves in the highest one-third range. This is expressed as:

$$P(H_*) = 1 - \frac{1}{3} = 1 - \exp\left(-\frac{H_*^2}{H_{rms}^2}\right), \tag{2.10}$$

which makes $H_* = 1.05H_{rms}$. From Equation 2.10, wave parameters can be calculated:

$$H_{r_{\frac{1}{3}}} = 4\sqrt{m_0} = 1.416H_{rms}, \tag{2.11}$$

$$H_{r_{\frac{1}{10}}} = 1.27H_{\frac{1}{3}} = 1.8H_{rms}, \tag{2.12}$$

$$H_{r_{\frac{1}{100}}} = 1.67H_{\frac{1}{3}} = 2.36H_{rms}. \tag{2.13}$$

Parameters $H_{r_{\frac{1}{10}}}$ and $H_{r_{\frac{1}{100}}}$ are useful in coastal engineering designs.

Note that Rayleigh distribution is good in narrow-band condition but not always true for shallow waters which deviate from it. Narrow-band condition means that if wave energy is concentrated in a very narrow range of wave period, the maxima of the wave profile will coincide with the wave crests and the minima of the troughs.

Another method in understanding the wave data is through the wave spectra. This method determines the distribution of wave energy and average statistics for each wave frequency by converting time series of the wave record into a wave frequency spectrum. This is usually done using the Fast Fourier Transform (FFT).

To better understand the wave spectrum through FFT, consider the wave surface profile of a single-amplitude and frequency wave given by:

$$\eta(t) = a\sin\omega t, \tag{2.14}$$

where a and ω are amplitude and angular frequency of sine wave. The variance of this over 2π is:

$$\sigma^2 = \overline{[\eta(t)]^2} = \frac{1}{2\pi}\int_0^{2\pi} a^2 \sin^2 \omega t d(\omega t), \tag{2.15}$$

$$\sigma^2 = \frac{a^2}{2} = 2\int_0^{\infty} S^1(\omega)d\omega = \int_{-\infty}^{\infty} S^2(\omega)d\omega, \tag{2.16}$$

where $S(\omega)$ is the wave spectrum.

Using these equations to apply for a random signal, the variance becomes:

$$\sigma^2 = \sum_{n=1}^{\infty} \frac{a_n^2}{2} = \int_0^{\infty} S(\omega)d\omega = m_0, \tag{2.17}$$

where m_0 is the zero-th moment of the spectrum. m_0 represents the area under the curve of $S(\omega)$.

The moments of the spectrum can be calculated by:

$$m_1 = \int_0^{\infty} \omega^i S(\omega)d\omega, \tag{2.18}$$

where $i = 0, 1, 2, ...$ From this, significant wave height from the wave spectrum can be calculated by:

$$H_{ws_s} = 4\sqrt{m_0}. \tag{2.19}$$

The sea surface spectrum is very difficult to approximate. Under certain conditions of the sea surface, the spectrum has a shape that can be parameterized [12]. The commonly used is the Pierson-Moskowitz or PM spectrum. This is a single parameter spectrum which assumes fully-developed seas. Fully developed sea means that a sea is produced by winds blowing steadily over hundreds of miles for several days. The equation of the PM spectrum is:

$$S(\omega) = \frac{0.0081g^2}{\omega^5} \exp\left(-0.74g^4(U_w\omega)^4\right), \tag{2.20}$$

where ω is the angular frequency and U_w is the wind speed at 19.5m above mean sea level. Wind speed is the parameter considered in this spectrum. Another popular spectrum is the Joint North Sea Wave Project or JONSWAP spectrum. In this study, this spectrum is utilized in the simulations to generate wave

data. This is an extension of PM with an assumption that seas do not fully develop and seas are fetch-limited. They added a peak enhancement factor, γ, to the PM spectrum. The JONSWAP spectrum is expressed as:

$$S(\omega) = \frac{\alpha g^2}{\omega^5} \exp\left[-\frac{5}{4}\left(\frac{\omega_p}{\omega}\right)^4\right]\gamma^r, \tag{2.21}$$

$$r = exp\left[\left(-\frac{(\omega-\omega_p)^2}{2\sigma^2\omega_p^2}\right)\right]. \tag{2.22}$$

The values for the constants in above equations:

$$\alpha = 0.076\left(\frac{U_{10}^2}{Fg}\right)^{0.22}, \tag{2.23}$$

$$\omega_p = 22\left(\frac{g^2}{U_{10}F}\right)^{\frac{1}{3}}, \tag{2.24}$$

$$\gamma = 3.3, \tag{2.25}$$

$$\sigma = \begin{cases} 0.07 & \omega \leq \omega_p \\ 0.09 & \omega > \omega_p, \end{cases} \tag{2.26}$$

where $g = 9.80665 m/s^2$, U_{10} is wind speed at height of 10m and F is the fetch.

The energy of the waves increases with fetch is calculated as:

$$\langle\zeta^2\rangle = 1.67 \times 10^{-7}\frac{U_{10}^2}{g}F. \tag{2.27}$$

2.2 Ocean Wave Monitoring Technologies

Technologies in ocean wave monitoring are evolving at same rate as other technologies. They are either solely created for ocean wave monitoring or commission along with other functions like detection. Generally, ocean wave monitoring technology is classified into two - in-situ and remote, however, there are systems that utilize both technologies.

(a) Ocean Wave Meteorological Buoys

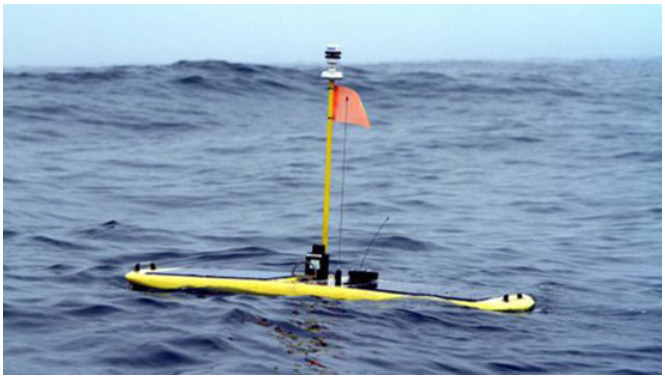

(b) Ocean Wave Gliders

Figure 2.2: In-situ Ocean Wave Monitoring Technology Devices

In-situ technology requires a more direct deployment of devices on the sea such as surface buoys, drifting buoys, underwater buoys, oceanographic vessels, towed vehicles, Autonomous Underwater vehicles (AUVs), Remote Operated Vehicles (ROVs), and surface gliders [13] [14] [15] [16] [17] [18] [19] [20] [21] [22] [23] [24] [25] [26] [27] [28] [29] [30]. The devices usually take point measurements and are highly accurate. The collected data closely represents the motions of the sea.

Remote technology uses long capturing devices such as HF radars and satellites which do not make physical contact to object measured. Unlike in-situ, devices can take wider area measurements [31] [32] [33] [34] [35]. The data collected are ensemble data within the area of interest.

There are also integrated wave monitoring technologies which combine in-situ

(a) Environment Monitoring Satellites

(b) High Frequency Radar

Figure 2.3: Remote Ocean Wave Monitoring Technology Devices

and remote devices in their systems [36] [37] [38] [39] [40] [41] [42] [43]. Compared to the in-situ, it has a better and wider coverage area. Compared to the remote, it can provide better resolution to the data. Since it collects data in both methods, it has comparative data which can lead to a more accurate data. Examples of such are the US Integrated Ocean Observing System (US-IOOS), Pacific Islands Ocean Observing System (PacIOOS) and Dart II System.

2.3 Ocean Wave Monitoring Technology Challenges

As with other emerging technologies, there are various challenges in ocean wave monitoring technologies. Each kind of wave monitoring technology provides both advantages and disadvantages.

In in-situ monitoring, it is limited to its deployment area. To extend its limited coverage, it needs multiple sensors deployed in the area of interest. This will enable the in-situ monitoring to provide an ensemble data. This issue creates another problem. More sensors could mean additional costs in the production and maintenance. Given in sophisticated in-situ monitoring systems, they usually have expensive in-situ devices hence an increase of number of sensors equates more expensive system. There is also an issue with the maintenance. Since this technology requires individual devices, maintaining each of them is a tedious task [44].

In remote monitoring, its limitation lies on its resolution. It is dependent on the coverage of the radars and satellites. Most environmental satellites can provide 1 kilometer resolution. This may not be enough for some applications. Also, since it deals with the operation of radars and satellites, special licenses and trainings are needed to operate the equipments. They are not easily accessible to an ordinary public or researcher. Operation and maintenance costs are also expensive for this technology.

Despite the advantages of the integrated monitoring, it still has a major disadvantage. Since it combines both technologies, production, installation, deployment, operation and maintenance are expensive. In most cases, it is the most expensive to build and use out of the three technologies.

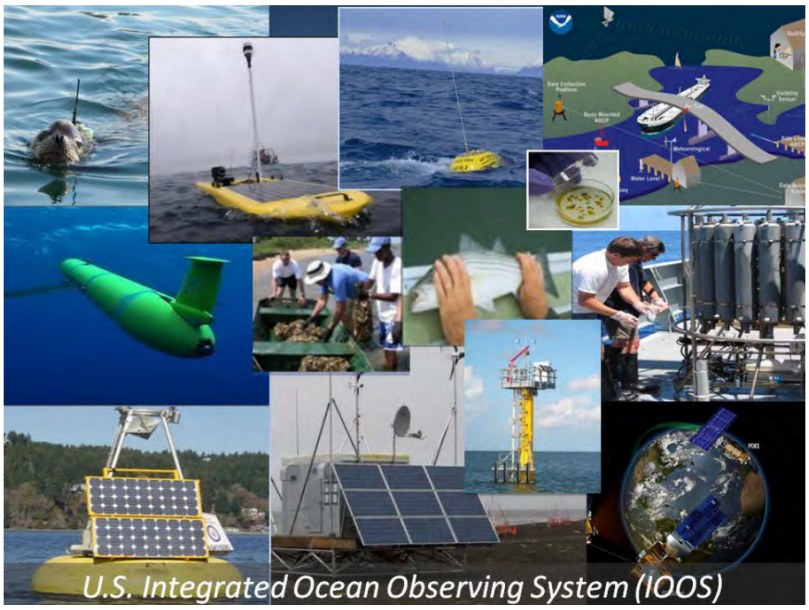

(a) US Integrated Ocean Observing System (US-IOOS)

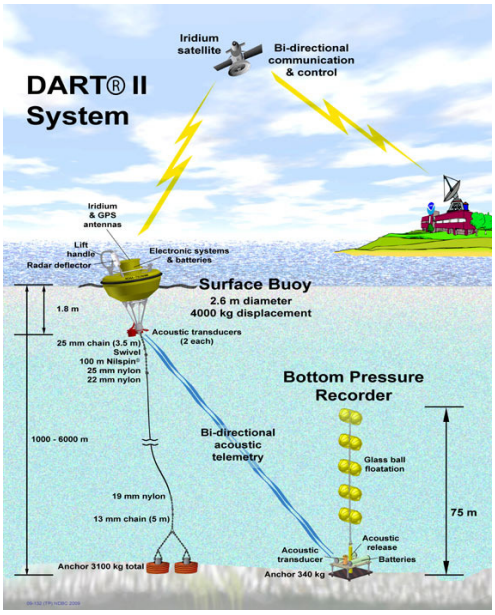

(b) Dart II System

Figure 2.4: Integrated Wave Monitoring Technologies

Also, most wave monitoring technologies utilize the conventional algorithms for the data processing which require long sets of data for accurate evaluation. Nowcasting is a challenge for in-situ because longer sets are needed in conventional algorithms hence it resorts to prediction models to generate approximations of the current wave conditions. It is also a challenge for remote because of its low resolution hence when it resorts to prediction models, its sparse data does not really help in giving accurate approximations of current wave conditions.

Chapter 3

System Overview of Ocean Wave Monitoring System Utilized

3.1 Definition of the Local In-situ Ocean Wave Monitoring System Utilized

The local in-situ ocean wave monitoring utilized in this study is a wireless network system of ocean wave sensors [5] [45]. This is an integrated monitoring system that monitors current wave conditions and reports wave information. Figure 3.1 shows the system diagram of the ocean wave monitoring system. This monitoring system is tested and deployed in different locations in the Philippines found in Figure 1.2.

3.2 Components of the System

The system consists of wave sensors and a central receiver. The wave sensors are deployed on seas while the central receiver is located on the shore or any place near the sea. The wave sensors are tasked to measure wave motions, gather wave data, do a pre-processing to the data and send the produced data evaluation to the central receiver. The central receiver receives the data sent by the modules.

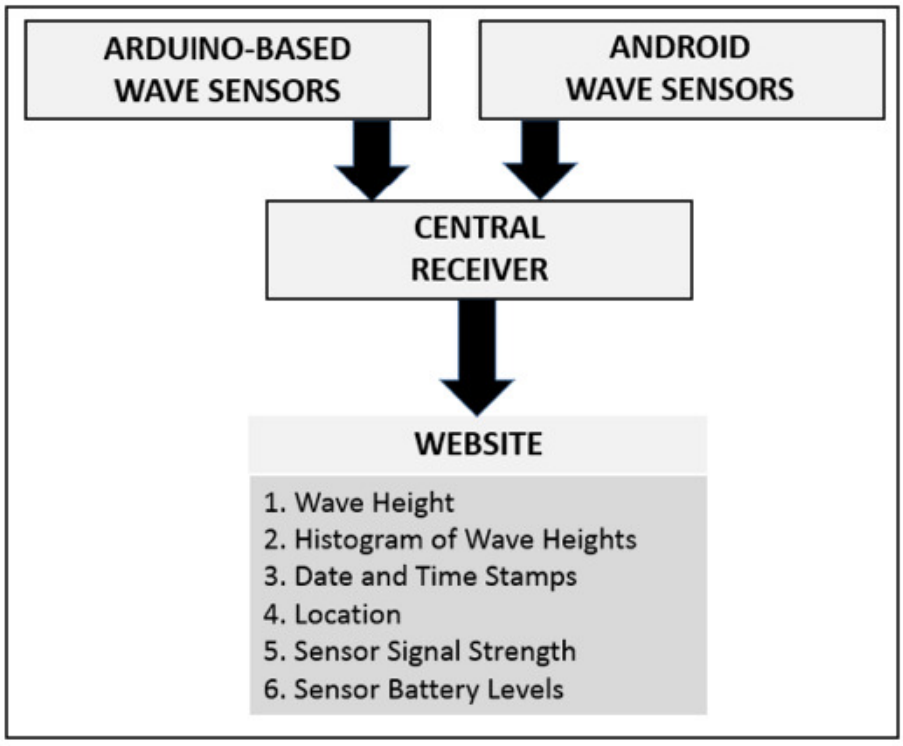

Figure 3.1: System Diagram of the Local In-Situ Ocean Wave Monitoring System

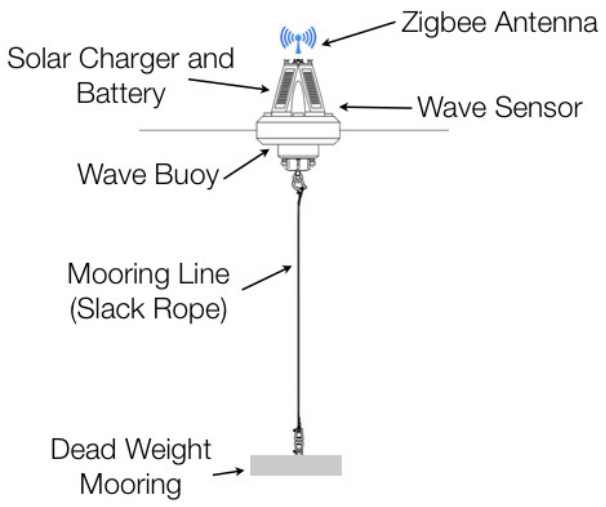

Figure 3.2: Configuration of a Deployed Wave Sensor

3.2.1 Wave Sensors

The wave sensors contain a sensor unit, processing unit, wireless communication module, battery and charging unit, and data storage unit. They are heavily waterproofed and mounted on a buoy or a floating platform. They are also moored through a slack rope to a dead-weight placed on the sea floor. This is to allow movements but at the same time, this fixes the wave sensor at a location. The configuration of the deployed wave sensors is shown in Figure 3.2.

They monitor the wave conditions through gathering of data. They can be programmed with various signal processing techniques to give them autonomy in distinguishing wave conditions before relaying the information to the central receiver. The pre-processing step ensures lesser but more accurate data and lesser traffic in the system. The processing techniques are explored heavily in this study. There are two kinds of wave sensors in this system. One is an arduino-based and the other is an android based wave sensor.

The arduino-based wave sensor in Figure 3.3(a) is built through the arduino open-source electronics prototyping platform based on easy-to-use hardware and software. The system diagram of the arduino-based wave sensor is shown in Figure 3.4.

The arduino board utilized for the wave sensors is the Arduino Pro. This micro controller board is based on the ATMega168. It requires 3.3V for power which is supplied by external LiPo battery with solar charger through the USB header and it runs at 8MHz. It has 14 digital input/output pins, 6 analog inputs, a battery power jack, a power switch, reset button, an ICSP header and pin headers. The micro controller has a 16KB Flash memory for storing code with 2KB used for bootloader. It has 1KB SRAM and 512 bytes of EEPROM. The microcontroller is programmed using the Arduino programming language based on Wiring and the Arduino development environment. For communication, the Arduino uses serial port (UART or USART). It communicates through the digital pins 0 for RX and 1 for TX as well as with the computer via USB. For the sensors, inertial measuring units (IMUs) are utilized which are connected to the microcontroller. The IMU contains an accelerometer and gyroscope sensors which together measure the relative change in positions of an object in 3D space as it moves [46]. To recall, a gyroscope is a device for measure orientation based on the principles of conservation of angular momentum. An accelerometer is a device that measures acceleration associated with the phenomenon of weight experienced by any test mass at rest in the frame of reference of the accelerometer device. Accelerometers are very sensitive to small vibrations and mechanical noise [47]. Through the aid of the gyroscope, accelerometer error can be corrected. Gyroscopes are less sensitive to linear mechanical movements. Since the microcontroller has limited memory, the storage unit is expanded through microSD. The user can opt for higher storage but for this wave sensor, only a 1GB microSD card is utilized. In order to connect the wave sensors to the sensor, wireless communication links are added. For the wireless communication links, Zigbee communication units are used. The arduino prototyping platform has ready to connect zigbee shields through which zigbee modules can be attached. Zigbee units allows one-to-one or peer-to-peer networks. It allows sending and receiving data with the standard arduino serial commands. The details of the Zigbee wireless communication unit are shown in Table 3.1.

The android-based wave sensor in Figure 3.3(b) consists of an android phone and a battery and charging unit. Android phones are generally well-equipped with embedded motion sensors such as accelerometers and gyroscopes and com-

Table 3.1: Zigbee Wireless Communication Unit Specifications (Xbee-Digi)

Parameter	Value
RF Data Rate	250 Kbps
Indoor/Urban Range	90m
Outdoor/RF Line-of-Sight Range	1500m
Transmit Power	10mW (+10dBm)
Receiver Sensitivity (1% PER)	-102dBm
Adjustable Power	yes
I/O Interface	3.3V CMOS UART, SPI, I2C, PWM, DIO, ADC
Configuration Method	API or AT commands
Frequency Band	2.4 GHz
Interference Immunity	DSSS
Serial Data Rate	1200 bps - 1Mbps
Antenna	Wire Whip
Encryption	128-bit AES
Reliable Packet Delivery	Retries/Acknowledgements
IDs and Channels	PAN ID, 64-bit IEEE MAC, 15 channels
Supply Voltage	2.7 - 3.6VDC
Transmit Current	205mA
Receive Current	47mA

munication modules such as GSM/3G which are suitable for the system. The android phone can be in any kind since there is an android application created for the system but for this system, it utilized HTC Wildfire and Samsung Galaxy Y. It sends processed data through text message to the central receiver.

3.2.2 Central Receiver

The central receiver receives all the data sent by the modules. It is a computer that has communication links connected to receive data. It has a zigbee explorer to receive data from the arduino wave sensor shown in Figure 3.5(a) and a gsm communication module to receive data from the android wave sensor shown in Figure 3.5(b). The central receiver is connected to the internet and it publishes

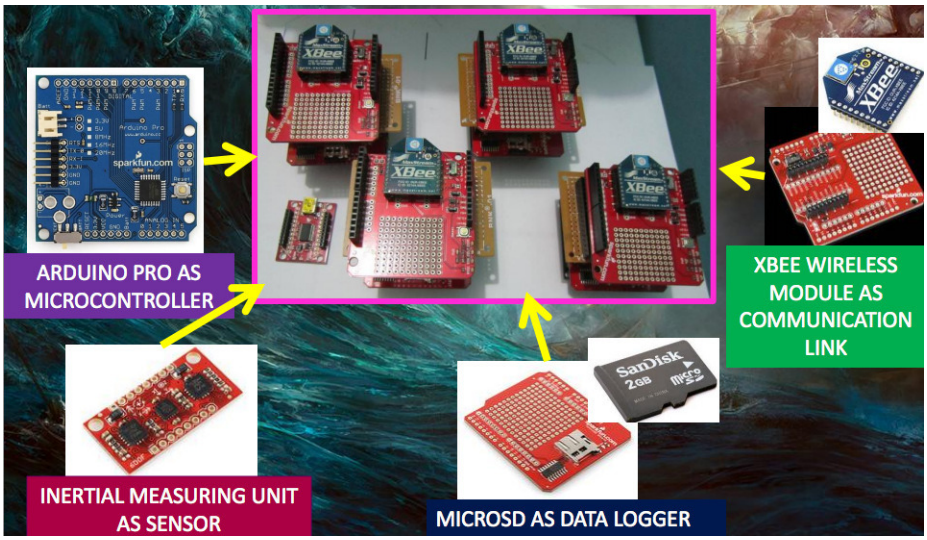

(a) Arduino-Based Wave Sensors and its components

(b) Android Based Wave Sensors and its components

Figure 3.3: Wave Sensors Utilized in the Local In-situ Ocean Wave Monitoring System

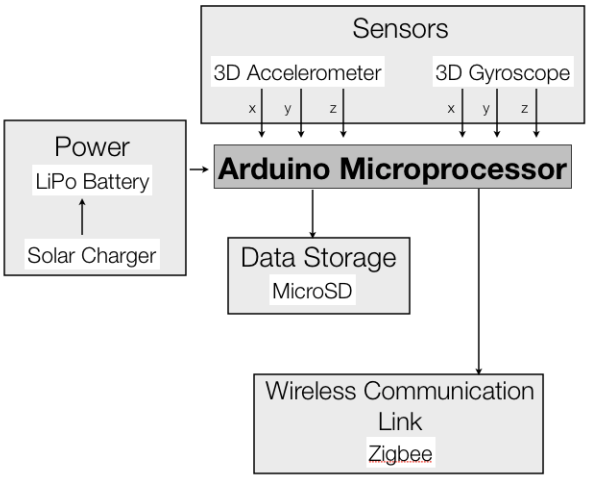

Figure 3.4: System Diagram of the Arduino-based Wave Sensor

data through a website.

3.2.3 Website

The website seen in Figure 3.6 publishes the data from all the sensors. It shows the wave height data, histogram of the wave height data, date and time stamps, location of each of the sensors, sensor signal strength and sensor battery levels. From the website, previous data from different locations can also be accessed.

3.3 Data Collected in the Local Ocean Wave Monitoring System

The wave sensors are tested in five different locations in the Philippines as shown in Figure 1.2(a). The data are sampled at 10Hz for 60 seconds. The wave sensors are equipped with six (6) types of data - 3 axis gyroscope data and 3 axis accelerometer data. These are utilized to correct the processing of vertical acceleration data. This process is thoroughly discussed in [47]. The examples of wave data from the experiments in the five locations are seen in Figures 3.7 to 3.11.

(a) Zigbee Explorer

(b) GSM Communication Module

Figure 3.5: Wave Sensors Utilized in the Local In-situ Ocean Wave Monitoring System

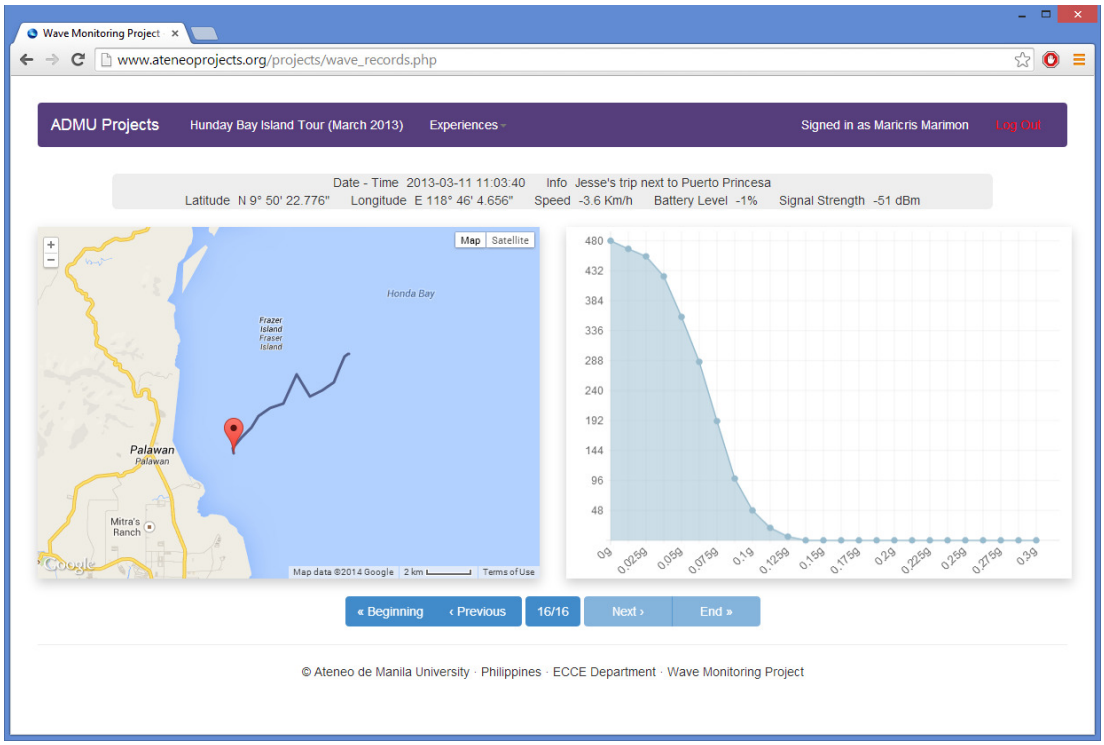

Figure 3.6: Screenshot of the Website of the Local In-situ Ocean Wave Monitoring System

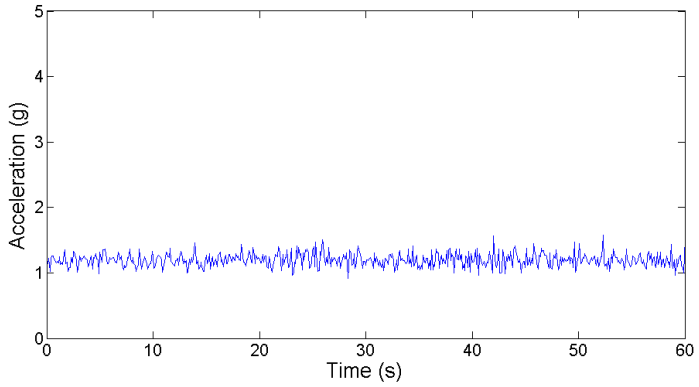

Figure 3.7: Acceleration data from Manila Bay Deployment

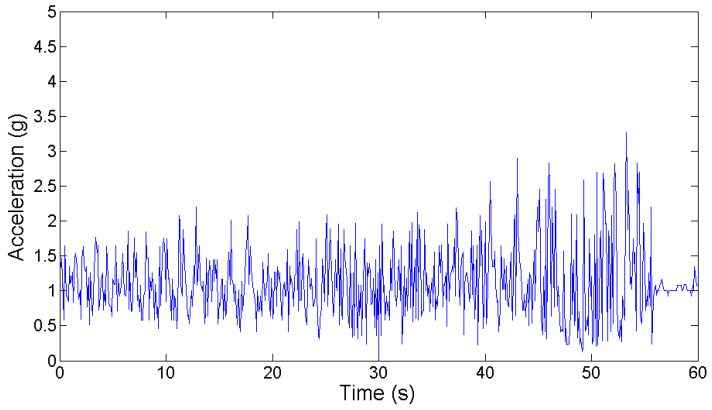

Figure 3.8: Acceleration data from Strait between Davao and IGACOS Deployment

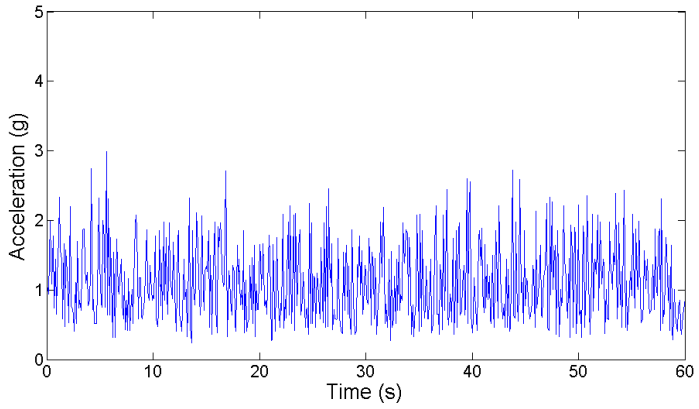

Figure 3.9: Acceleration data from Davao Coast near IGACOS Deployment

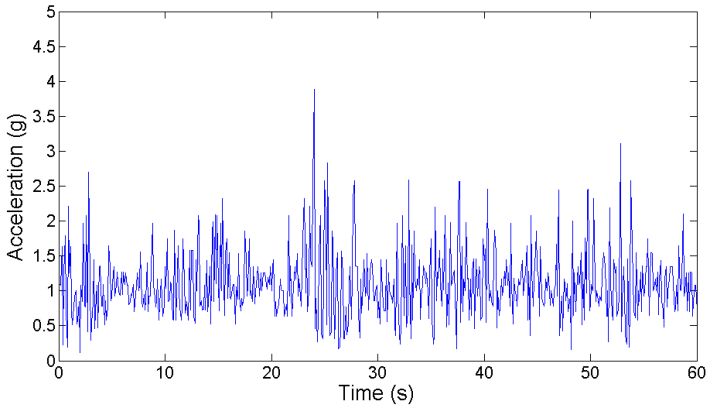

Figure 3.10: Acceleration data from IGACOS Coast near Davao Deployment

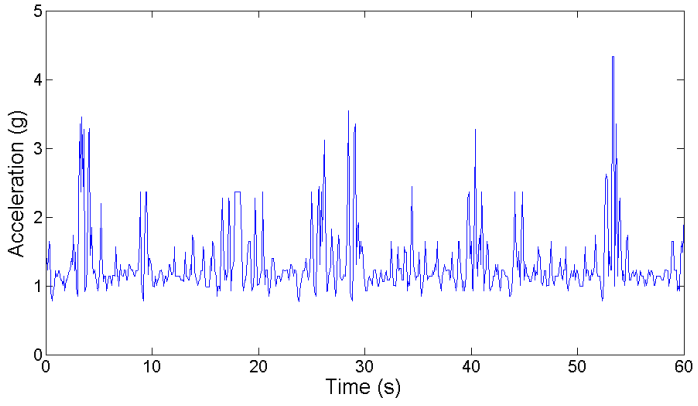

Figure 3.11: Acceleration data from Davao Coast far from IGACOS Deployment

Chapter 4

Detection of Severe Wave Conditions

This section presents the first aim of the study which is to enable the local ocean wave monitoring system to detect severe ocean wave conditions. Severe wave conditions indicate that there are harsh wind systems around the area of interest or in very rare occurrences, tsunami events. For this study, it does not distinguish the two events.

In the wave monitoring system, the wave sensors which are deployed on seas are given the task and autonomy to discern wave conditions before relaying information to the central receiver. In order to do this, processing techniques are programmed in the wave sensors. These processing techniques assess the short time series data and recognize whether the data indicate severe wave conditions.

In this chapter, two processing techniques are explored for the detection of severe wave conditions. First is the thresholding technique and the second one is the statistical analysis technique.

4.1 Threshold Technique

Threshold technique is a signal processing method which the wave sensor counts the events at which the gathered values exceed the value of the threshold criterion [45]. This comes from the idea that when a condition exceeds the expected regular condition, it signifies an abnormality. The main mechanism of this technique is

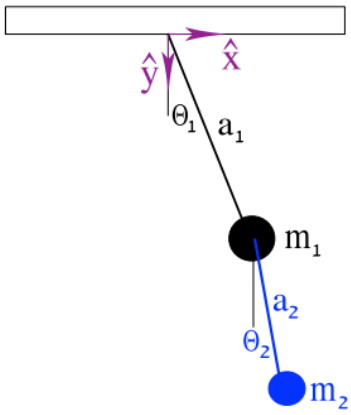

Figure 4.1: Double Pendulum suspended at a fixed point in the ceiling with the axes at the upper end of each rod allow for frictionless rotation in the plane. The upper mass is m_1 and the lower is m_2. The lengths of the rods are a_1 for upper and a_2 for lower.

that all generated values are compared to a certain threshold value. If current value exceeds the threshold value, it will be counted as a crossing. If there is a crossing detected, the count number is increased. This process is repeated until the programmed sampling is over. After the sampling duration, the count number is compared again to the acceptable count number. If this exceeds the acceptable count number, the wave sensors sends this data to the central receiver.

Since this technique relies on a threshold value, choosing the proper threshold value is important. It defines the sensitivity which the wave sensor evaluates and identifies the severe wave conditions. The threshold criterion utilized for the wave sensors are taken from the double pendulum experiments. Double pendulum is a simple mechanical system that has two simple pendula attached end to end that exhibits nonlinear behavior [48] [49]. This system is utilized for simulating wave conditions because it is difficult to get actual severe wave conditions. Since double pendulum machine exhibits nonlinear behavior, it is assumed in [5] that it closely resembles actual wave conditions as shown in Figure 4.2.

The double pendulum consists of two particles, of masses m_1 and m_2, connected by two light rods of lengths a_1 and a_2, respectively, which are connected as shown in Figure 4.1. In the double pendulum set up, there are parameters

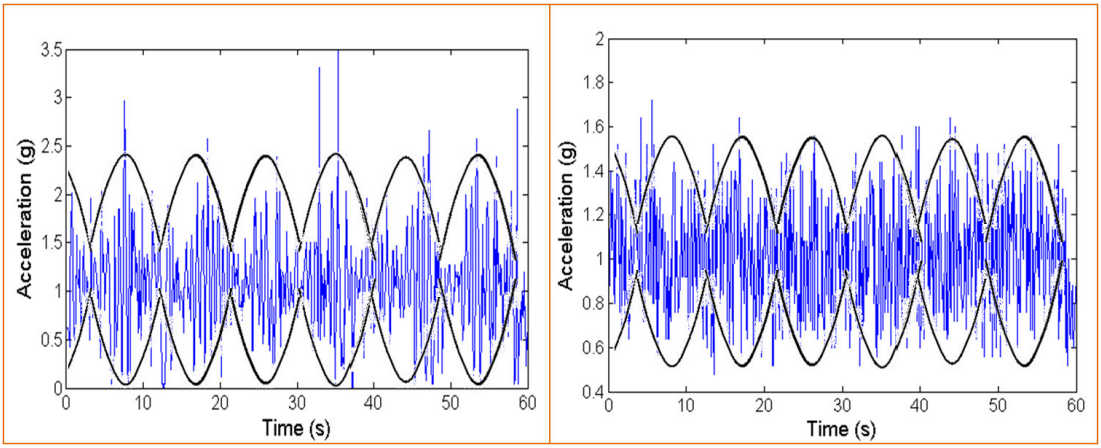

Figure 4.2: Comparison of the double pendulum dynamics and actual wave dynamics in acceleration

that are varied to create different types of motions. For the experiments, the parameters - a_2 and θ_2 are changed. It was discovered in several experiments that changing these two parameters generated significant changes in the motions. The monitoring of the motion is done by attaching a sensor on m_2. Also, to ensure that the two masses are equal, an additional mass is added to m_1 so that it will be equal to m_2.

The double pendulum is set to simulate abnormal wave conditions expected in ocean waves. For the first wave condition, the length a_2 is set to 20cm and the angle ϕ_2 is set to 30 degrees. For the second condition, the length is 40cm and the angle is 60 degrees. Table 4.1 shows the number of data points at corresponding acceleration values. It can be observed that the second wave condition generated larger acceleration as compared to the first wave condition hence, it can represent a severe wave condition. As mentioned before, setting the threshold influences the sensitivity of the wave sensor. It is shown in Figure 4.3 that the number of data points exceeding the threshold varies as the threshold criterion is varied.

Based from the double pendulum experiments, it is sufficient to set threshold levels at $1g$, $1.5g$ and $2g$ where g=$9.8m/s^2$. Figures 4.4 to 4.5 shows the resultant acceleration plotted with the three threshold levels. The figures show that when threshold is increased, fewer crossings are detected. Table 4.2 shows the values of the count number at each threshold value. Note that the wave data have 600

Table 4.1: Number of data points per acceleration value range

Acceleration Value Range (g)	Wave Condition 1 $l = 20$cm, $\theta_2 = 30$ deg	Wave Condition 2 $l = 40$cm, $\theta_2 = 60$deg
-1 to -0.5	0	1
-0.5 to 0	0	1
0 to 0.5	36	90
0.5 to 1	262	197
1 to 1.5	258	206
1.5 to 2	31	78
2 to 2.5	12	20
2.5 to 3	1	5
3 to 3.5	0	1
3.5 to 4	0	1

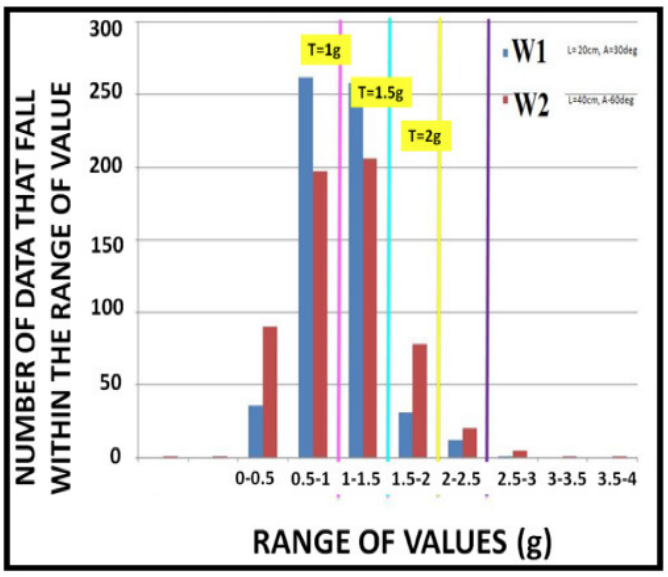

Figure 4.3: Histogram of data points per acceleration value with threshold set at 1g, 1.5g, 2g

Table 4.2: Count of crossings at each threshold value

Acceleration Threshold Value	Count Number
T = 1g	336
T = 1.5g	99
T = 2g	35

instantaneous values for 1 minute sampling duration. If the count exceeds 50 percent of the total number of instantaneous values then that current wave data are considered to have a severe condition. At this kind of wave condition, the wave sensor reports to the central receiver that it has detected a severe wave condition. Larger counts signifies more severe wave condition. As mentioned before, the threshold value defines the sensitivity of the wave sensor. This value can be set according to the user's preference.

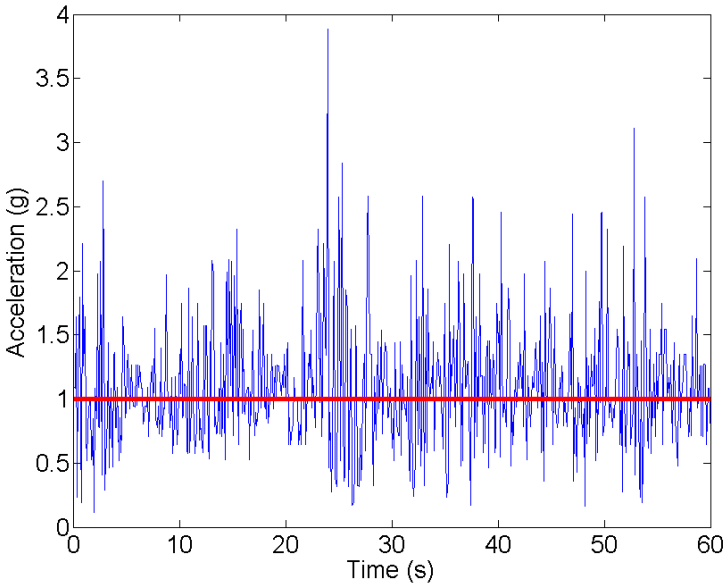

Figure 4.4: Resultant acceleration of sensor node with threshold set at 1g

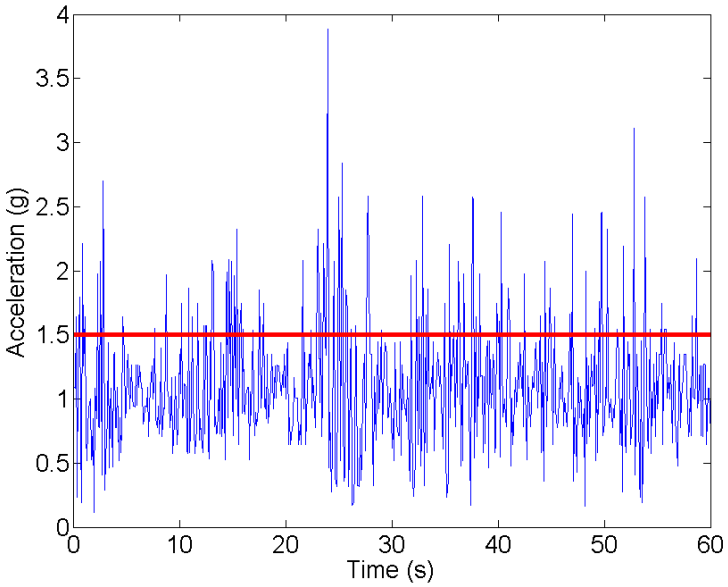

Figure 4.5: Resultant acceleration of sensor node with threshold set at 1.5g

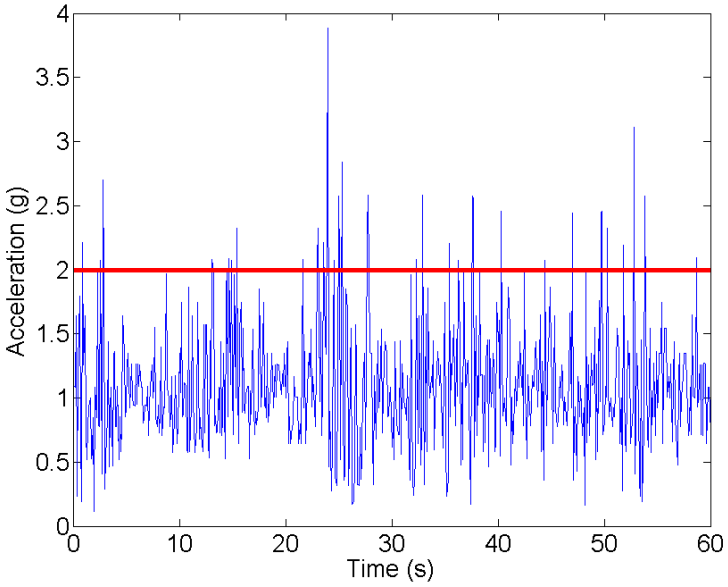

Figure 4.6: Resultant acceleration of sensor node with threshold set at 2g

4.2 Statistical Analysis Technique

In the previous technique, processing the data is quite straightforward because it compares each instantaneous data with the fixed threshold criterion. It is easy to apply as long as the threshold criterion is chosen well. Despite of its simplicity, there are many disadvantages in setting up the threshold criteria. The threshold criteria are determined by the acceleration values generated from the simulated abnormal wave conditions on the double pendulum machine. This is not so favorable because the values are too rigid. Actual wave conditions can vary according to the coastal characteristics of the deployment location. Values for normal wave conditions in a location might be higher than the other locations hence setting fixed threshold criterion for all the wave sensors might not be so practical and effective. Assessment of wave conditions should be associated with the local normal wave conditions in a specific area [50] [51].

In order to generate these values, the statistics of the wave heights from normal conditions are utilized. A statistical wave distribution is generated from the wave heights. Significant wave height which is the average of the highest one third of the waves [52], is normally extracted from the distribution but in this study, higher order statistics are utilized. The higher order statistics considered to be utilized are the kurtosis and skewness. These two statistical parameters describe the shape of the distribution which closely accounts the wave record. Outliers, which signify severe wave conditions, can also be observed and detected by means of determining the shape of the distribution. Kurtosis and skewness are also good indicators of nonlinearity. The probability density function (pdf) of the waves with higher order interactions between the component waves considered is given as:

$$p(\eta) = \frac{1}{\sqrt{2\pi m_0}} e^{-\frac{\eta^2}{2m_0}} (1 + \frac{1}{6}\lambda_3 H_3 + (\frac{1}{24}\lambda_4 H_4 + \frac{1}{72}\lambda_3^2 H_6) + ...) \tag{4.1}$$

where m_0 is the variance, H_i represents hermite polynomials and λ_3 and λ_4 are associated with skewness and kurtosis. This equation 4.1 is just a probability function density of a normal distribution multiplied by a nonlinear factor

wherein the parameters skewness and kurtosis are included. This shows that by considering the nonlinear theory of ocean waves, skewness and kurtosis have to be accounted for hence setting skewness and kurtosis values as comparative values is a good course of action in improving the previous signal processing method.

This signal processing technique is different from the previous method since it utilizes wave height data. To have wave height data, data transformation is needed. The acceleration data gathered from the wave sensors are converted to wave height by integrating twice. After the conversion, the skewness and kurtosis values are calculated from the wave height data. It is expected that locations may have different values for normal conditions. It is important that the wave sensor gather several data and collate the possible average values for kurtosis and skewness on a specific area. These values are considered as values for normal wave conditions in the area. From these values, the severity of the new wave conditions introduced to the locations are evaluated.

For each new wave data, skewness and kurtosis are calculated and compared to the comparative values. If the new wave data generate higher values, this signifies that the new wave condition is severe. The higher the difference, the more severe is the wave condition.

Another difference of this technique to the previous technique is that it requires gathering of data for the whole sampling duration before processing the data. This refrains the wave sensor to constantly make decision at every instantaneous data. However, this second technique is still similar to the first because it utilizes certain values to compare and evaluate the present conditions.

By definition, kurtosis is the measure of whether the distribution is peaked or flat. It is given as:

$$Kurtosis = \frac{\sum_{i=1}^{N}(H_i - \overline{H})^4}{(N-1)\sigma^4} \tag{4.2}$$

where H_i is the wave height, $\overline{H}$ is the mean wave height, σ is the standard deviation and N is the number of data points.

The higher kurtosis value, the more peaked is the distribution at a specific point. It means that higher kurtosis signify that there is a significant number of readings that fall at specific value. If that specific value is large, it would mean that there are large amplitude waves in the wave record.

Table 4.3: Wave Height Statistics from the Five Locations

	DATA	Kurtosis	Skewness
1	Manila Bay	3.2106	0.1889
2	Strait between Davao and IGACOS	2.0859	0.0357
3	Davao Coast near IGACOS	3.1035	0.2073
4	IGACOS Coast near Davao	3.7276	0.1704
5	Davao Coast far from IGACOS	8.5712	1.9068

Skewness is the measure of the vertical symmetry of the distribution of the wave heights. Positive skewness means that there is an elongated tail to the higher values. It is given as:

$$Skewness = \frac{\sum_{i=1}^{N}(H_i - \overline{H})^3}{(N-1)\sigma^3} \tag{4.3}$$

where H_i is the wave height, $\overline{H}$ is the mean wave height, σ is the standard deviation and N is the number of data points.

If both parameters have high and positive values, the observed condition is abnormal. It indicates that there are frequent occurrences of high amplitude waves.

To test this technique, the raw acceleration data from the wave sensors in the five locations are transformed into wave height time series data. After the transformation, statistical wave height distribution is generated. Kurtosis and skewness are then extracted and shown in Table 4.3.

Based from Table 4.3, most of the locations show kurtosis higher than 3 and skewness greater than 0. Note that values of kurtosis and skewness for normal distribution are 3 and 0 respectively. Typically coastal areas have higher values for kurtosis and skewness as compared to deeper seas. This is because landforms influence interaction of the waves.

The conventional circular path of water particles, shown in Figure 4.7, which

is followed by the buoy, is deformed to an elliptical shape which produces white caps. White caps produces indiscernible sea pattern due to polychromatic ocean waves. White caps can also be seen in areas experiencing strong wind systems. Since there are more waves that have different amplitudes and frequencies, the kurtosis and skewness values are expected to be higher than the Gaussian values. Locations 1, 3, 4 and 5 exhibit these characteristics. It is interesting to observe that location 2 has lower kurtosis and skewness as compared to the other locations. This is because this location is not a coastal area and is in deeper waters. In contrast, location 5 has high kurtosis and positively skewed. This shows that this coast experiences larger waves due to access of open seas. Open seas are more prone to entry of random waves from nearby storms [53]. This is opposite to location 1, a sheltered bay, which has rock formations that limit the entry of these random waves. Locations 3 and 4 have similar range of values due to wave reflections since they are opposite coasts of a strait.

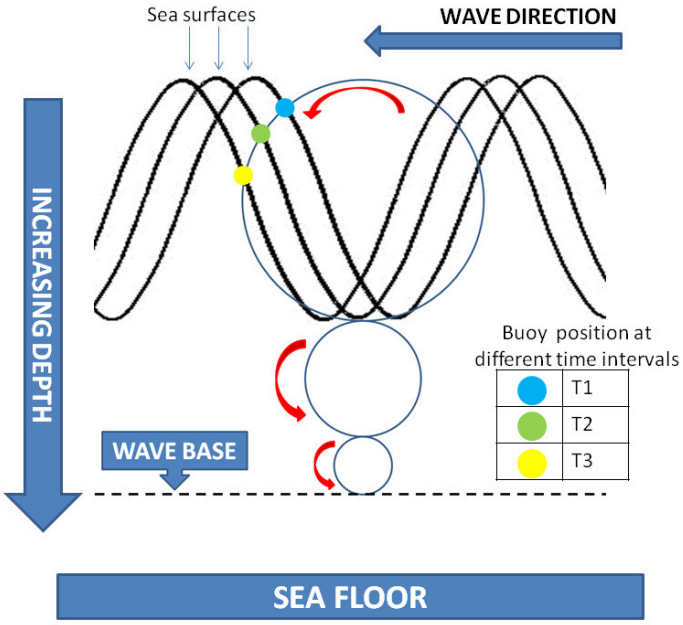

Figure 4.7: Circular path of water particles

Since the kurtosis and skewness values are already generated from the locations, these can now be used as comparative values to the wave sensors. In order

Table 4.4: Differences of the statistical parameters of the two new sets of data from the baseline data generated from the locations

		Difference	
	LOCATION	Kurtosis	Skewness
Simulated			
Waves	2	1.7795	0.8789
K = 3.8654	3	0.7619	0.7073
S = 0.9146	4	0.1378	0.7442
Actual Wave			
Data	2	2.6517	0.90167
K = 4.7376	3	1.6341	1.07327
S = 0.86597	4	1.01	1.03637

to test these values, the kurtosis and skewness values are calculated from the two test data - the simulated severe condition wave data and the actual wave data from a severe condition. The kurtosis and skewness values of locations 2, 3, 4 are used in the comparison and evaluation since the second set of data is gathered within these areas.

The difference of the kurtosis and skewness values from each of the comparative value to the new test data are calculated and shown in Table 4.4. From Table 4.4, it can be observed that the two test data have significant differences from the normal kurtosis and skewness values particularly the second test data. This signal processing technique considers wave data as severe when the kurtosis and skewness values exceed 50% than the location's values for normal wave conditions. In these two tests, locations 2 and 3 detected the abnormality for the second test data since this test data has values that are 50% higher than their normal values.

Based from the results of the statistical analysis technique, it has successfully detected severe wave conditions. This technique offers better and improved way in the detection since it considers the deployment location and the normal values of waves expected in the location. There are times that a normal condition in a particular area might be different from another location due to bathymetry

and by considering this, the technique avoids false or inaccurate detection. This technique is also better than the previous method because it processes data at specific time hence it limits the need to utilize the system's resources.

Chapter 5

Processing of Data From Multiple Sensors

5.1 Blind Signal Deconvolution through Independent Component Analysis

The local in-situ ocean wave monitoring considered for this study has multiple wave sensors. Each wave sensor collects data for a predetermined sampling duration. The second aim of this study is to separate the signals coming from the multiple wave sensors. This section presents the technique that deals with signal separation.

In theory as presented in Chapter 2, ocean waves are linear superposition of waves that have different amplitudes and phases. If a sensor gathers wave data at a specific point, the wave data are mixtures of these waves. These individual waves are considered as source signals and the gathered wave data are the observed signals in this context. There is no a priori information about these waveforms or polarizations of the source signals and the mixing system hence it is difficult to retrieve these source signals from the wave data without resorting to blind signal deconvolution (BSD) methods.

Blind signal deconvolution method is used to recover input signal of a dynamical system (mixer) from its output signal but a striking feature is that both the system and the input are unknown[54]. Under a set of assumptions, the recovery

is usually achieved by adjusting an inverse system (demixer) based on statistical independence of the signal. In order to make statistically independent signals, independent component analysis is utilized.

Consider the input (source) signal $u(t) = (u_1(t), \cdots, u_m(t))^T$, which is a vector-valued function of discrete-time $t = 1, \cdots, T$. Assume that the components of $u(t)$ are random variables with the following properties; zero mean, spatially and temporally independent, identically distributed, and at most one of them is Gaussian distribution [55].

Suppose that the observe output signal is

$$y(t) = G * u(t), \tag{5.1}$$

where G is the impulse response of a dynamical system (mixer) and $*$ denotes discrete-time convolution.

The z-transformation of G is denoted by $G(z)$ with the same symbol. Assume that $G(z)$ is unknown but a square, biproper rational, and stable transfer matrix of minimal phase. By this assumption, $y(t) = (y_1(t), \cdots, y_m(t))^T$; i.e., it has the same dimension as $u(t)$, and $G(z)^{-1}$ is also a stable rational matrix.

The objective is to recover the source signal $u(t)$ from $y(t)$ (shown in Figure 5.1) observed for a certain period (hence this is a batch processing), in the following sense: connect a tunable filter $H(z)$ whose output is $\hat{u} = (\hat{u}_1(t), \cdots, \hat{u}_m(t))^T$, and adjust $H(z)$ so that the components of $\hat{u}(t)$ are as independent as possible (a criterion is minimized). It is known that after minimization:

$$H(z)G(z) = P\Lambda(z),$$

$$\Lambda(z) = \operatorname{diag}\left(\alpha_1 z^{-\nu_1}, \ldots, \alpha_m z^{-\nu_m}\right),$$

for some permutation matrix P, scalars α_i, and integers ν_i $(i = 1, \ldots, m)$. This means that the resulting $\hat{u}$ is a recovery of u within indeterminacy of scalar multiplication, permutation, and time lag.

The above indeterminacy is typical in BSD. If this is removed via prior knowledge, then $H(z)$ plays a role of inverse system, and hence $G(z)$ can be identified in this sense.

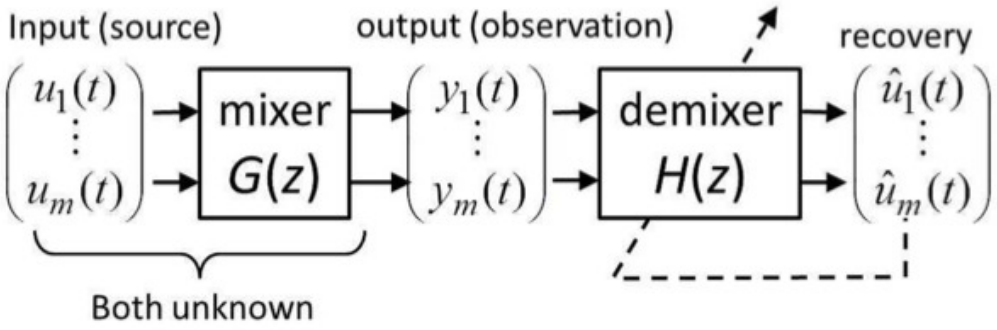

Figure 5.1: Problem of blind signal deconvolution

There are several schemes for blind signal deconvolution. A well-known scheme for BSD is based on FIR (Finite Impulse Response) approximation of the demixer.

This scheme considers the state space representation

$$x(t+1) = Ax(t) + By(t) \tag{5.2}$$

$$\hat{u}(t) = Cx(t) + Dy(t) \tag{5.3}$$

where

$$A = \begin{pmatrix} O_m & \cdots & O_m & O_m \\ I_m & & 0 & \vdots \\ & \ddots & & O_m \\ 0 & & I_m & O_m \end{pmatrix}, B = \begin{pmatrix} I_m \\ O_m \\ \vdots \\ O_m \end{pmatrix}, \tag{5.4}$$

$$C = \begin{pmatrix} H_1 & H_2 & \cdots & H_L \end{pmatrix}, \qquad D = H_0. \tag{5.5}$$

Note that A and B have a special structure that makes $H(z) = C\left(zI - A\right)^{-1} B + D$ an FIR filter.

On the other hand C and D have nontrivial block elements which will be adjusted.

Figure 5.2 is a block diagram of this FIR filter, where z^{-1} denotes one step delay and L is the number of taps. The parameters $H_i (i = 0, 1, \ldots, L)$ are adjusted so that the components of $\hat{u}$ is independent. Based on the Kullback Leibler Divergence of $\hat{u}$ and the above system representation, this is achieved by minimizing the cost function:

$$\ell(\hat{u}, H) = -\log |\det(D)| - \sum_{i=1}^{m} \log q_i(\hat{u}_i), \tag{5.6}$$

where $q_i(\cdot)$ is the probability density function of the source signal u_i. Since these are unknown, replace them with some suitable function is done.

The function $\ell(\hat{u}, H)$ is non-negative and is equal to zero if and only if signals $\hat{u}$ are mutually independent. Hence, the objective is to find H which minimizes this cost.

Since it is impossible to obtain the optimal solution analytically, resorting to a gradient descent algorithm is done. The update law based on the gradient of parameter is described by

$$\Delta C(k) = -\eta(k)\varphi(\hat{u})\, x^{\mathrm{T}}, \tag{5.7}$$

$$\Delta D(k) = \eta(k)\left(I_m - \varphi(\hat{u})\, y^{\mathrm{T}} D^{\mathrm{T}}(k)\right) D(k), \tag{5.8}$$

where k denotes the iteration time and $\eta(k) > 0$ is a learning rate, and $\varphi(\hat{u})$ is the score function.

The function $\varphi(\hat{u}_i) = \tanh(\hat{u}_i)$ is used, if the distribution of the random variable $\hat{u}_i$ is super-Gaussian, while $\varphi(\hat{u}_i) = \hat{u}_i^3$ is used, if $\hat{u}_i$ is sub-Gaussian.

The FIR scheme is effective in signal deconvolution however it requires a large number of parameters. In standard identification schemes, parameters space of a dimension given by prior knowledge is set and then adjust the parameter by the input/output behavior. This is in contrast to signal processing methodology, which motivated others and the present author in developing BSD schemes that fit into system identification. Tanaka et al. developed a scheme that represents the demixer via polynomial matrix fraction of a given order and derived a learning law by projecting the FIR learning law onto the polynomial coefficient space. The

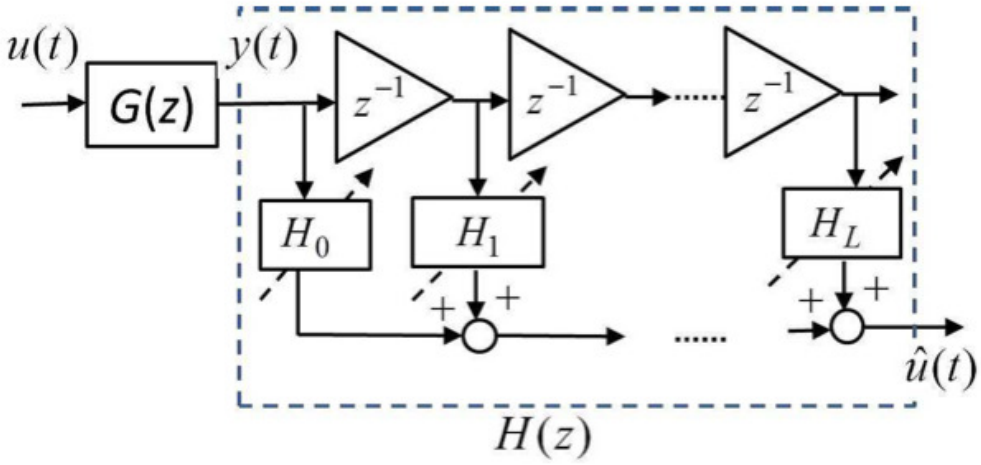

Figure 5.2: Demixer by FIR filter

projection is given by solving a certain set of linear equation in every iteration.

Instead of (5.4) and (5.5), the demixer is

$$H(z) = D(z)^{-1}N(z), \tag{5.9}$$

where

$$D(z) = I_m + D_1 z^{-1} + \cdots + D_p z^{-p}, \tag{5.10}$$
$$N(z) = N_0 + N_1 z^{-1} + \cdots + N_q z^{-q}. \tag{5.11}$$

This is called right fractional representation by polynomial matrices. The degrees p and q are given from prior knowledge and not so large in practical situations. Figure 5.3 shows a block diagram of the demixer. Note that this is an IIR filter.

The learning law in this case is derived by projecting that by FIR approximation. Let

$$\mathcal{D} := (D_1 \ \cdots \ D_p), \quad \mathcal{N} := (N_0 \ N_1 \ \cdots \ N_q)$$

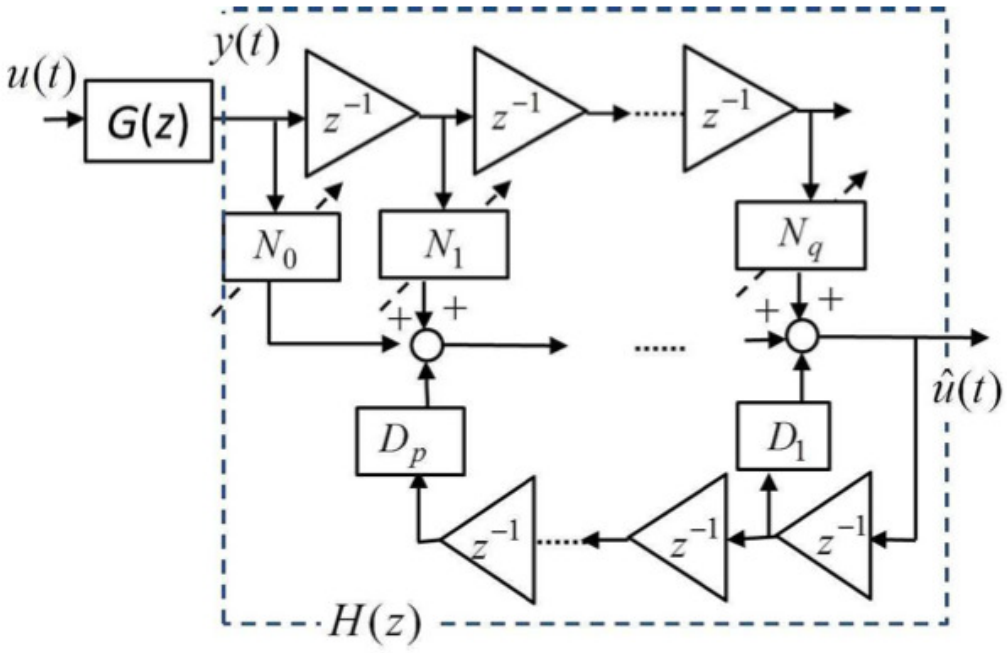

Figure 5.3: Demixer by IIR filter

Then the update law is given by

$$
\begin{aligned}
&(\mathcal{D}, \mathcal{N}) \to (\mathcal{D} + \Delta\mathcal{D}, \mathcal{N} + \Delta\mathcal{N}) \\
&\Delta\mathcal{D} = -(I_m \quad \mathcal{D})\Delta\mathcal{H}_R \cdot \mathcal{H}_R^T(\mathcal{H}_R\mathcal{H}_R^T)^{-1} \\
&\Delta\mathcal{N} = (I_m \quad \mathcal{D})\Delta\mathcal{H}_L + \Delta\mathcal{D} \cdot \mathcal{H}_L,
\end{aligned}
$$

where

$$(\mathcal{H}_L \ \mathcal{H}_R) = (H_0 \ H_1 \ \cdots H_L). \tag{5.12}$$

$\Delta\mathcal{H}_L$ and $\Delta\mathcal{H}_R$ are given by FIR learning scheme. Though this scheme is effective, it is indirect since it resorts to the same FIR learning law utilized in Zhang et al.

Because there are some disadvantages in the two previous schemes, an improvement is developed [56]. A new learning law is derived.

The improved scheme adopts the demixer $H(z)$ in the right fractional representation (5.9) and computes the gradient of the coefficients more directly than the previous projection scheme.

It starts by considering how the estimation $\hat{u}$ (i.e., output of $H(z)$) is affected when $H(z)$ is changed. If $H \to H + dH$, then

$$\begin{aligned} d\ell &= \ell(\hat{u}, H + dH) - \ell(\hat{u}, H) \\ &= -\mathrm{tr}(dH_0 H_0^{-1}) + \varphi^T(\hat{u}) d\hat{u}, \end{aligned} \tag{5.13}$$

$$\varphi(\hat{u}) = \begin{pmatrix} \varphi_1(\hat{u}_1) \\ \vdots \\ \varphi_m(\hat{u}_m) \end{pmatrix}, \tag{5.14}$$

$$\varphi_i(\hat{u}_i) = -\frac{d}{d\hat{u}_i} \log\, q_i(\hat{u}_i) = -\frac{q_i'}{q_i}, \tag{5.15}$$

where φ_i is called the score function.

In Zhang et al., $H(z)$ is adjusted with an FIR filter (namely A and B are in the special form and not adjusted), hence

$$d\hat{u} = dCx + dH_0 y + C dx$$

with x being the state vector.

On the other hand, in this framework, the parameters in (5.10), (5.11) are adjusted. From (5.9), there is $D(z)H(z) = N(z)$ hence, $dD(z)H(z) + D(z)dH(z) = dN(z)$. Therefore,

$$\begin{aligned} d\hat{u} &= dH(z) y \\ &= D(z)^{-1} (dN(z)\ dD(z)) \begin{pmatrix} I \\ -H(z) \end{pmatrix} y. \end{aligned} \tag{5.16}$$

Observing that $z^{-\tau}y(t) = y(t-\tau)$ for $\tau = 1, 2, \cdots$,

$$d\hat{u}(t) = D(z)^{-1}(dN_0 \cdots dN_q \; dD_1 \cdots dD_p)\xi(t), \tag{5.17}$$

$$\xi(t) := \begin{pmatrix} y(t) \\ \vdots \\ y(t-q) \\ \hat{u}(t-1) \\ \vdots \\ \hat{u}(t-p) \end{pmatrix}.$$

The right-hand side of (5.17) contains $D(z)^{-1}$, which means that this is again IIR filter. Namely, by means of the power series expansion

$$D(z)^{-1} = \Delta_0 + z^{-1}\Delta_1 + \cdots =: \Delta(z),$$

(5.17) can be rewritten as

$$d\hat{u}(t) = \sum_{\tau=0}^{\infty} \Delta_\tau (dN_0 \cdots dN_q \; dD_1 \cdots dD_p)\xi(t-\tau). \tag{5.18}$$

In actual calculation without much loss of accuracy the above infinite summation can be truncated up to some finite number of terms, say $\tau = 20$. The above formula can be substituted to (5.13) and observe that $N_0 = H_0$. Now recall that, in general, if $df = a^T dX b$ for a matrix differential dX and column vectors a, b, then

$$\frac{\partial f}{\partial X} := \left(\frac{\partial f}{\partial x_{ij}}\right) = ab^T.$$

Here, note the order of multiplication.

Therefore,

$$\begin{aligned}
\frac{\partial \ell}{\partial N_0} &= -N_0^{-T} + \varphi(\hat{u}(t))y^T(t) \\
&\quad + \Delta_1^T \varphi(\hat{u}(t))y^T(t-1) + \cdots \\
\frac{\partial \ell}{\partial N_1} &= \quad \varphi(\hat{u}(t))y^T(t-1) \\
&\quad + \Delta_1^T \varphi(\hat{u}(t))y^T(t-2) + \cdots \\
&\vdots \\
\frac{\partial \ell}{\partial D_1} &= \quad \varphi(\hat{u}(t))\hat{u}^T(t-1) \\
&\quad + \Delta_1^T \varphi(\hat{u}(t))\hat{u}^T(t-2) + \cdots
\end{aligned}$$

Note that Δ_τ can be obtained as follows. By definition, $D(z)\Delta(z) = I$ hence,

$$\begin{aligned}
&\Delta_0 = I \\
&D_1 + \Delta_1 = 0 \\
&D_2 + D_1\Delta_1 + \Delta_2 = 0 \\
&D_3 + D_2\Delta_1 + D_1\Delta_2 + \Delta_3 = 0 \\
&\vdots
\end{aligned}$$

Thus,

$$\Delta_\tau = -D_\tau - \sum_{\nu=1}^{\tau-1} D_{\tau-\nu}\Delta_\nu, \tau = 1, 2, \cdots \tag{5.19}$$

The above result gives the learning law for reducing mutual information $\ell(\hat{u}, H)$. Initializing the adjusting parameter of the demixer as

$$D(z) = I \quad \text{and} \quad N(z) = I \tag{5.20}$$

Then the renewal law is given by

$$\begin{aligned}
\delta N_0 &= \eta(k)\left(N_0^T - \varphi(\hat{u}(t))y^T(t)\right. \\
&\qquad \left. -\Delta_1^T\varphi(\hat{u}(t))y^T(t-1) - \cdots\right) \\
\delta N_1 &= \eta(k)\left(-\varphi(\hat{u}(t))y^T(t-1)\right. \\
&\qquad \left. -\Delta_1^T\varphi(\hat{u}(t))y^T(t-2) - \cdots\right) \\
&\vdots \\
\delta D_1 &= \eta(k)\left(-\varphi(\hat{u}(t))\hat{u}^T(t-1)\right. \\
&\qquad \left. -\Delta_1^T\varphi(\hat{u}(t))\hat{u}^T(t-2) - \cdots\right) \\
&\vdots
\end{aligned}$$

for small learning rate $\eta(k) > 0$.

Note that this is writen as "on-line learning." Theoretically "batch process learning" based on the expectation E is more appropriate. In actual calculation, resorting to "time average" instead of using E is done.

There is another improvement of the third BSD scheme [57] [58]. This improvement arise because in the third BSD it deals with the $D(z)^{-1}$ which involves power series expansion. This method is sometimes difficult to treat. In the improved third scheme, the time signal is $v(t)$ is computed as:

$$v := D^T(z^{-1})^{-1}\varphi(\hat{u}) \tag{5.21}$$

or in time domain, starting at $t = T_f$ (final time), computing in reverse time:

$$\begin{aligned}
v(t) := D_1^T v(t+1) - \cdots - D_p^T v(t+p) \\
+\varphi(\hat{u(t)}), sp, t = T_f, T_f - 1, \cdots
\end{aligned} \tag{5.22}$$

For simplicity, $v(t) = 0$ for $t > T_f$. Note that these values remain finite for

any large T_f because $D(z)$ is Hurwitz. The update law is given by:

$$\begin{aligned}\delta N_0 &= \eta(k)\left(N_0^{-T} - [v(t)y^T(t)]_t\right)\\ \delta N_q &= -\eta(k)\left[v(t)y^T(t-q)\right]_t\\ \delta D_p &= \eta(k)\left[v(t)\hat{u}^T(t-p)\right]_t\end{aligned}$$

for small learning rate $\eta(k) > 0$.

The proof of the above scheme is as follows. For a vector time sequence $\{f(t)\}_{t=0}^{\infty}$, consider its z-transform $\tilde{f}(z) := \sum_{t=0}^{\infty} f(t)z^{-t}$. For $f, g \in \ell_2$, the inner product is defined as:

$$\langle f, g\rangle := \sum_{t=0}^{\infty} f^T(t)g(t). \tag{5.23}$$

where $\langle ., .\rangle$ represents sesquilinear form.

Given the lemma,

$$\langle f, g\rangle = \frac{1}{2\pi}\int_0^{2\pi} \tilde{f}^*(e^{j\omega})\tilde{g}(e^{j\omega})d\omega \tag{5.24}$$

where $*$ denotes the complex conjugate transposition.

To prove this, consider:

$$\tilde{f}(z^{-1})\tilde{g}(z) = \sum_{-\infty}^{\infty} a_t z^t, \tag{5.25}$$

where $a_0 = \langle f, g\rangle$ and for any nonzero integer $t \neq 0$

$$\int_0^{2\pi} e^{j\omega t}d\omega = 0 \tag{5.26}$$

and this completes the proof.

A proposition is presented that for $f, g \in \ell_2$ and a stable transfer matrix H(z):

$$\langle f, Hg\rangle = \langle H^\sharp f, g\rangle \tag{5.27}$$

where $Hg = \mathcal{Z}^{-1}[H(z)\tilde{g}(z)]$ and $H^\sharp f = \mathcal{Z}^{-1}[H^T(z^{-1})\tilde{f}(z)]$ are written with slight abuse. $H^\sharp$ is an adjoint of H. This can be seen as a generalization of the adjoint matrix of a square matrix which has a similar property involving the standard complex inner product.

The proof is given by lemma:

$$\langle f, Hg\rangle = \int_0^{2\pi} \tilde{f}^*(e^{j\omega})H(e^{j\omega})\tilde{g}(e^{j\omega})d\omega \tag{5.28}$$

$$= \int_0^{2\pi} (\tilde{f}^*(e^{j\omega})H^T(e^{j\omega})\tilde{g}(e^{j\omega}))^* d\omega \tag{5.29}$$

$$= \int_0^{2\pi} (\tilde{g}^*(e^{j\omega})H^T(e^{-j\omega})\tilde{f}(e^{j\omega}))^* d\omega \tag{5.30}$$

$$= \langle g, H^\sharp f\rangle = \langle H^\sharp f, g\rangle \tag{5.31}$$

To test the algorithms, source signals are simulated. Source signals $u = (u_1, u_2)^T$ are M-sequence or pseudorandom binary signal $u_i(t) \in \{-1, 1\}$, for $i = 1, 2$ and $t = 1, \ldots, 2^{13} - 1 = 8191$ (or $2^7 - 1 = 127, 2^10 - 1 = 1023$). Figure 5.4 shows the source signals but showing only 1st to 100th samples for optimal viewing of the data.

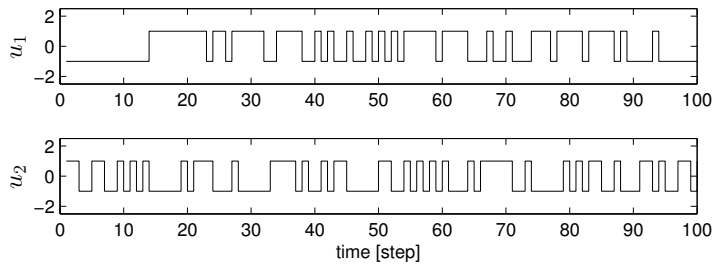

Figure 5.4: Source Signals for ICA

Next, in order generate the observed signals which are representative of sensor signals, the source signal is fed through a mixer.

Consider the transfer matrix

$$G(z) = \bar{D}^{-1}(z)\bar{N}(z) \tag{5.32}$$

with

$$\bar{D}(z) = \begin{pmatrix} 1.00 & 0.00 \\ 0.00 & 1.00 \end{pmatrix} + \begin{pmatrix} 0.40 & -0.70 \\ 0.70 & 0.40 \end{pmatrix} z^{-1} \tag{5.33}$$

$$\bar{N}(z) = \begin{pmatrix} 1.00 & 0.00 \\ 0.00 & 1.00 \end{pmatrix} + \begin{pmatrix} -0.50 & -0.60 \\ 0.60 & -0.50 \end{pmatrix} z^{-1} \tag{5.34}$$

which is to be identified. This is stable and minimum phase, and its pole-zero map and impulse response are given in Figs. 5.5 and 5.6, respectively. The poles are $-0.40 \pm j0.70$ and the zeros are $0.50 \pm j0.60$. Note that the system is vibrative to some extent.

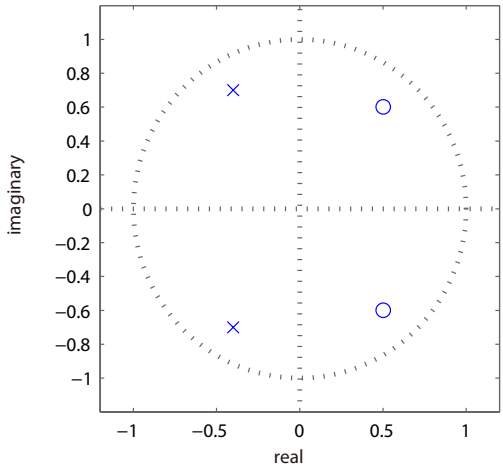

Figure 5.5: Pole Zero Map of the Mixer

This is regarded as the mixer. The observed signal is observed as:

$$y = G(z)u \tag{5.35}$$

as shown in Figure 5.7. The simulation conditions for the experiments are shown in Table 5.1.

The FIR method by Zhang, IIR method by Tanaka and the author's method are applied to the observed signals. Figures 5.8 to 5.10 give the recovered signals from the three methods respectively. Figure 5.11 shows the error between

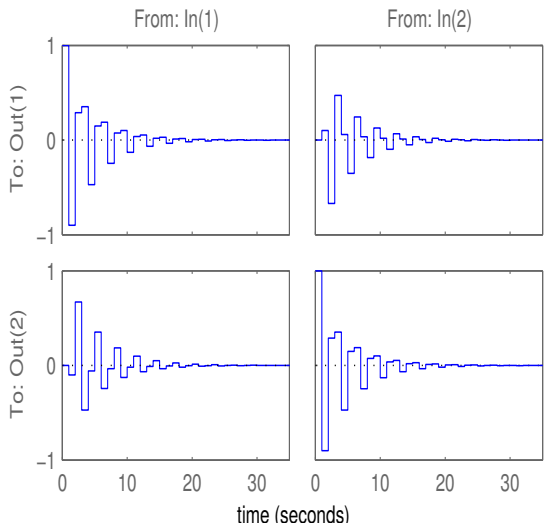

Figure 5.6: Mixer Impulse Response

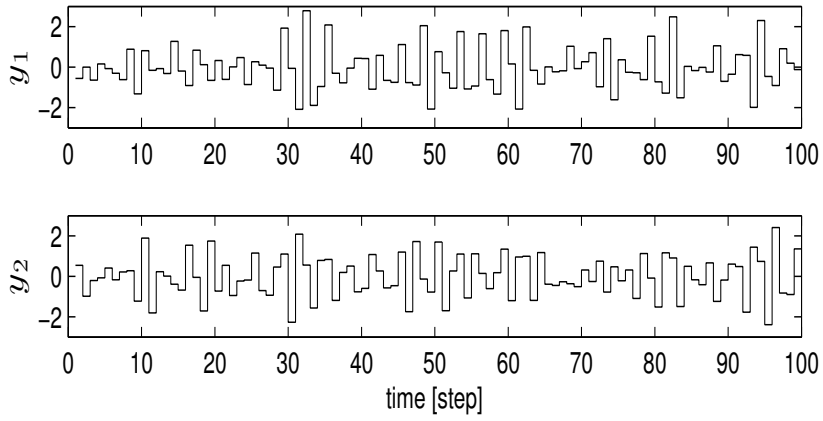

Figure 5.7: Observed Signals

the source and recovered signals. The recovery errors by the third method are significantly smaller than those generated by the conventional FIR method by Zhang and the IIR method by Tanaka. Figure 5.12 shows the comparison of the three methods in the test for dependency of RMSE after learning on the sample number. It is observed that the third method has the lowest RMSE in the three different sample numbers with the same iteration. Figure 5.13 shows the RMSE versus the number of iteration. This also shows that out of the three methods,

Table 5.1: Simulation Conditions

Parameter	Value
Number of samples	1023 (unless otherwise stated)
Number of iterations	2000 (unless otherwise stated)
Learning rate η	0.005
Number L of taps in FIR approximation	30

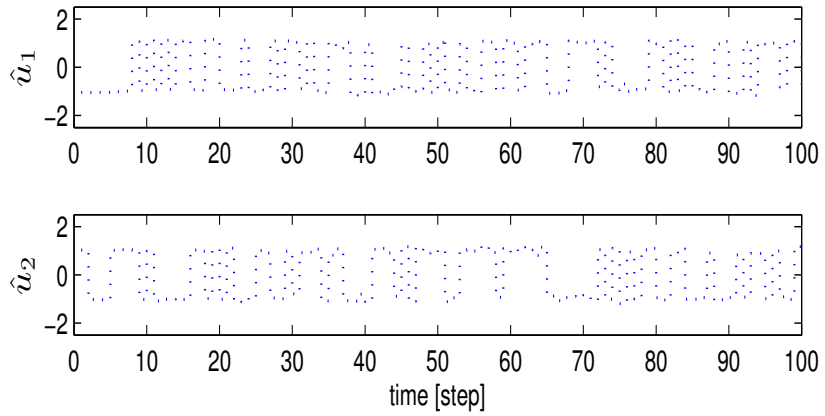

Figure 5.8: Recovered Signals by FIR Approximation Scheme [2]

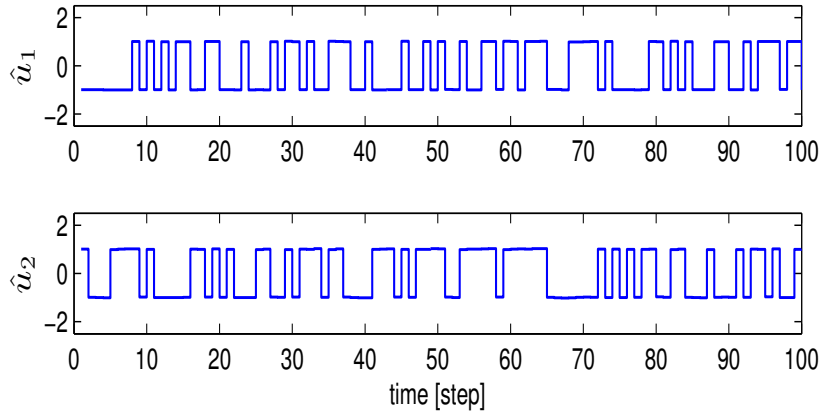

Figure 5.9: Recovered Signals by projected IIR Scheme [3]

the third one converges faster. The accuracy for blind identification is also tested by means of Bode diagrams of the mixer. This is shown in Figure 5.14. At first

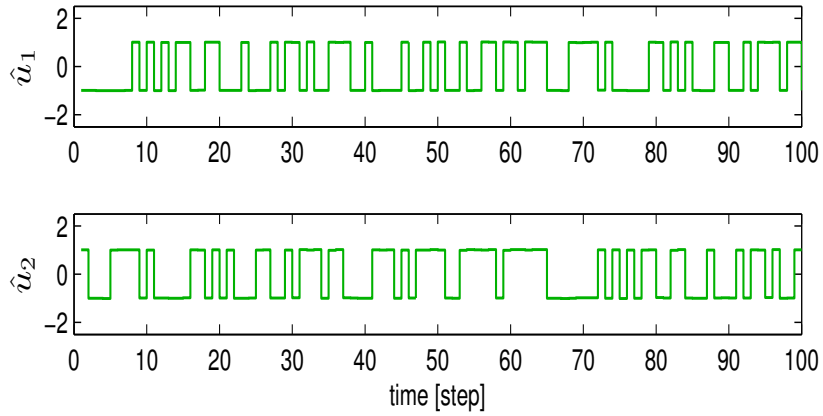

Figure 5.10: Recovered Signals by Improved Scheme

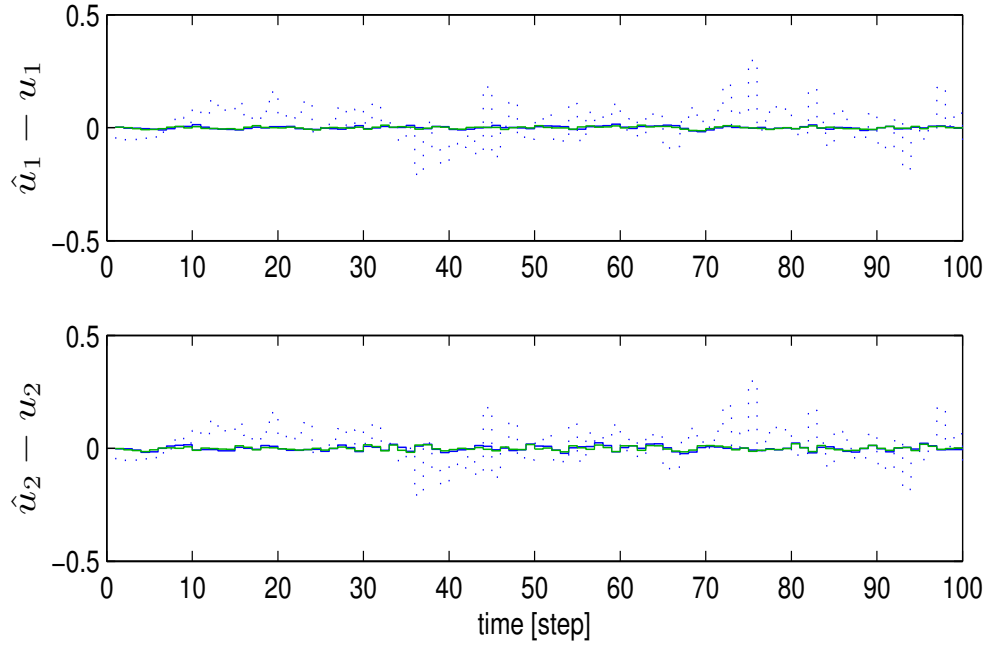

Figure 5.11: Error between the source and recovered signals (blue (dotted): FIR approximation, blue (solid): Projected IIR, green (solid): First Improved Scheme)

sight it appears that the upper right phase plot fives different results, but the phase difference is 360 degrees hence they are same in reality. This means that the identified systems are fairly close to the true value for all the methods. Note that all of the methods in this section are sufficiently iterated up to 5000.

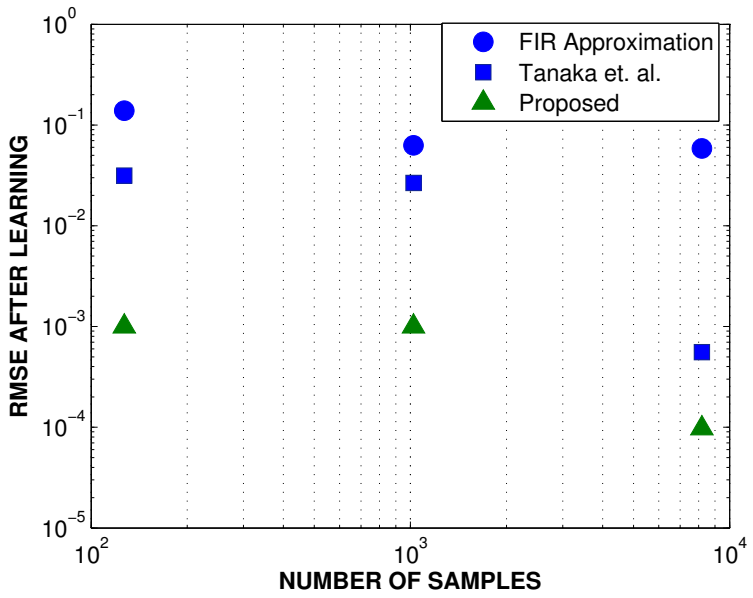

Figure 5.12: RMSE after learning vs. Number of Samples

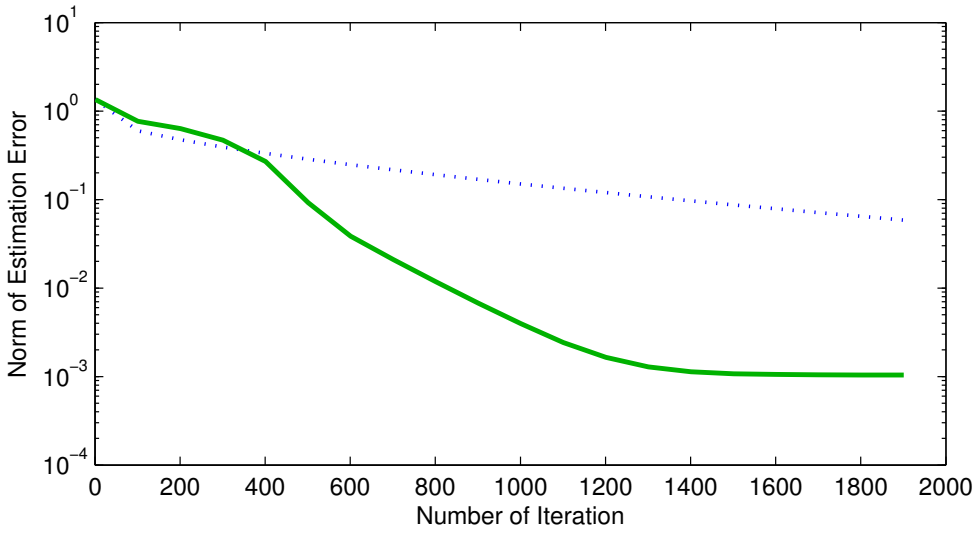

Figure 5.13: RMSE versus iteration (blue (dotted): FIR approximation, green (solid): Improved Scheme)

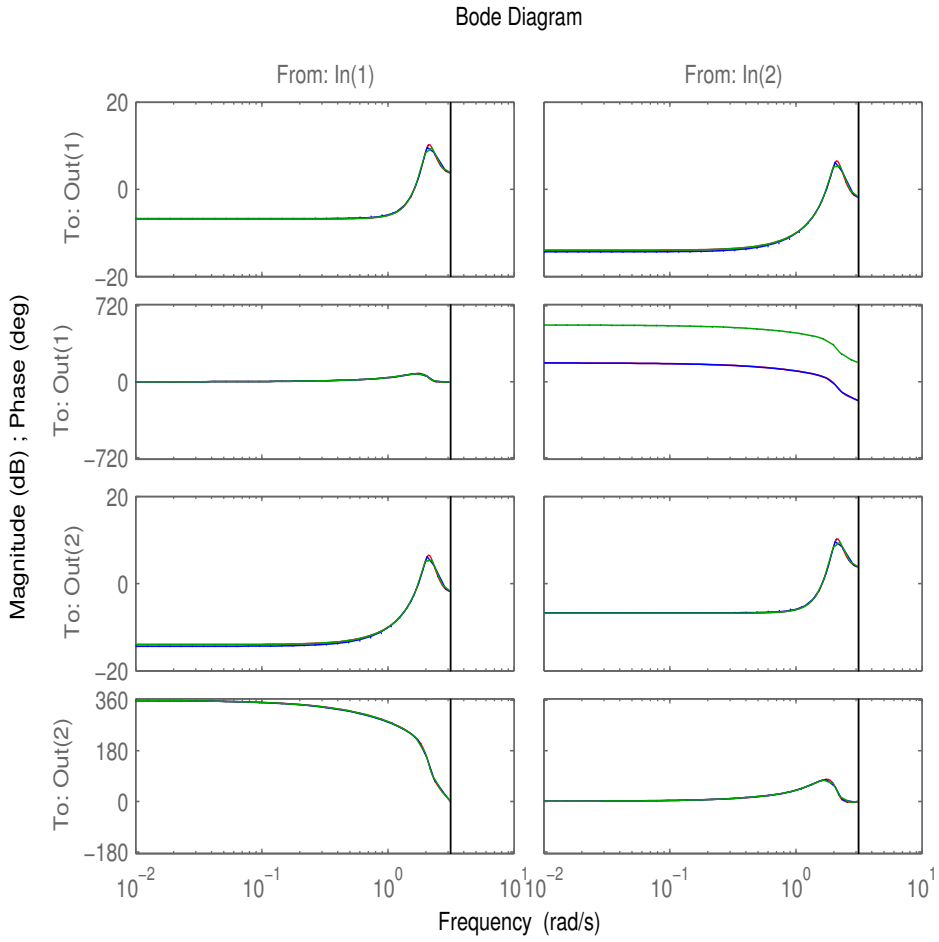

Figure 5.14: Bode Diagram of $G(z)$ (red: true, blue (dotted): FIR approximation, blue (solid): Projected IIR, green (solid): Improved Scheme)

Seeing the good performance of the third BSD scheme, a test to its improvement is done to compare its performance with the two BSD schemes. The same mixer is utilized shown in Figure 5.5 and the input (source) signals $u = (u_1, u_2)^T$ are M-sequence (pseudo random binary signal) $u_i(t) \in \{-1, 1\}$, for $i = 1, 2$ and $t = 1, \cdots, 2^{13} - 1 = 8191$ as shown in Figure 5.15. The output signal, $y = G(z)u$ is shown in Figure 5.16. Figures 5.17 - 5.19 show the recovered signals from the conventional scheme, Tanaka et. al. scheme and the further improved third scheme. Figure 5.20 shows the error versus the iteration. It can be observed

from this graph that the further improved third method has a significantly lower RMSE as compared to the two schemes. Also, the scheme converges faster than the two.

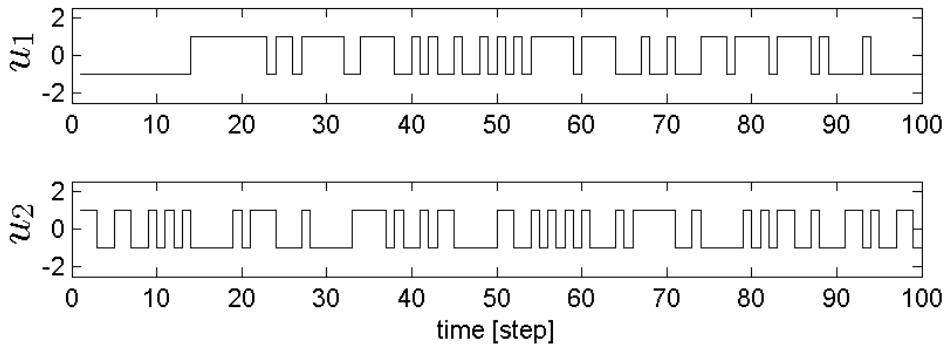

Figure 5.15: Source Signals

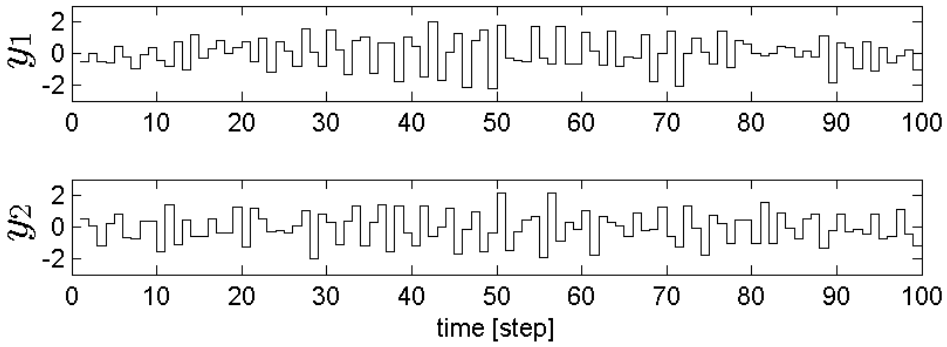

Figure 5.16: Observed Signals

Based from all the results, the proposed techniques have successfully recovered the signals from the mixed observed signals. These are helpful in recovering signals from multiple sensors in the system. At this point in the study, only simulated data are utilized in the BSD techniques. Using real wave data are yet to be explored in the future works of this study.

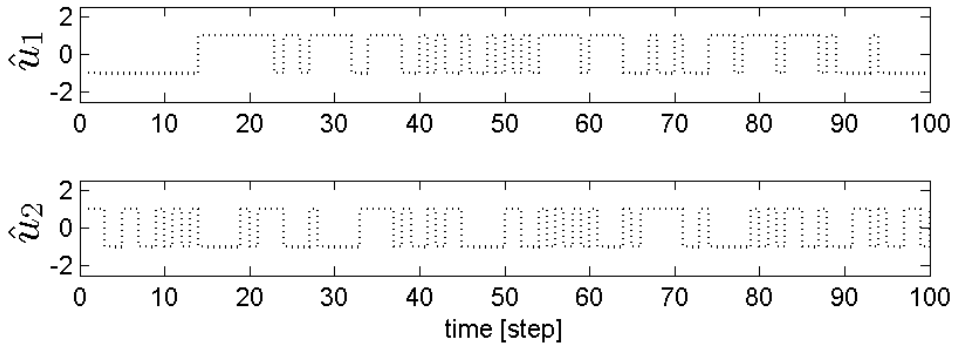

Figure 5.17: Recovered Signals from Conventional Scheme

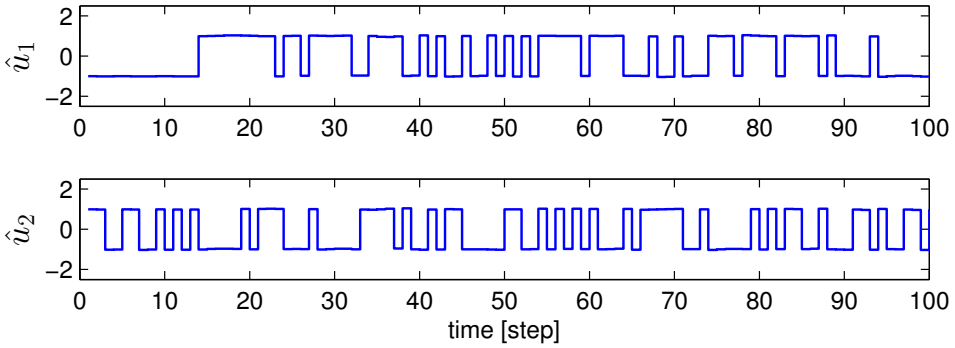

Figure 5.18: Recovered Signals from Tanaka et. al Scheme

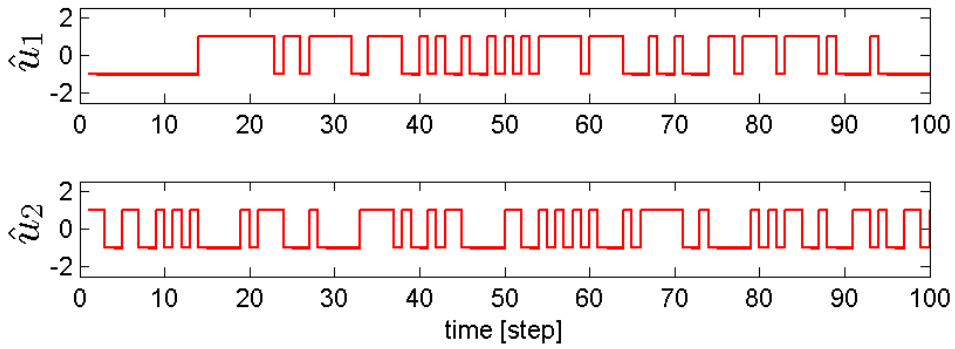

Figure 5.19: Recovered Signals from Further Improved Third Scheme

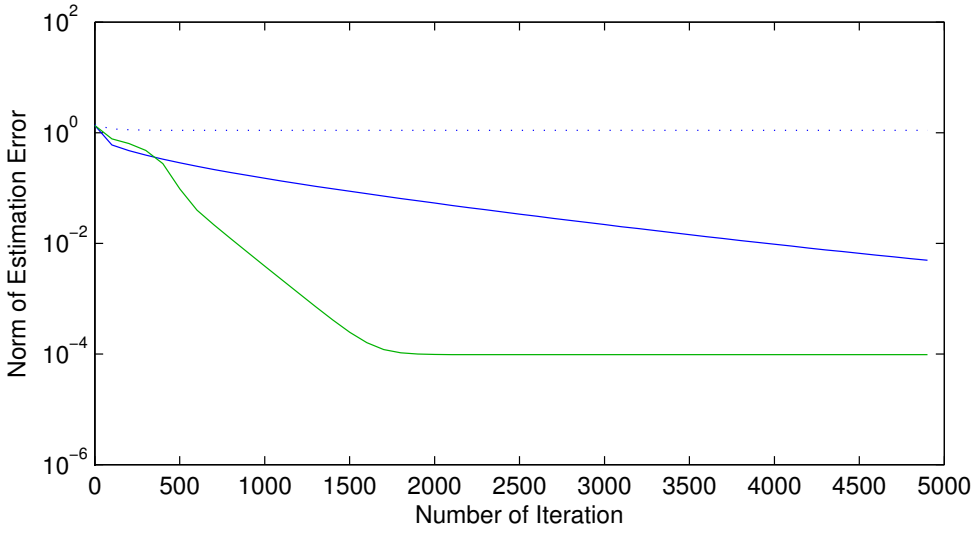

Figure 5.20: RMSE versus iteration (blue (dotted): FIR approximation,blue (solid): Tanaka et. al., green (solid): Further Improved Third Scheme)

Chapter 6

Classification of Wave Conditions

In this section, the third goal of this study is explored. Detection of wave conditions is practical in wave monitoring systems as they provide information about the current wave conditions however, the information sometimes are not so sufficient. The eventual goal of a wave monitoring system is to be able to classify wave conditions given the gathered data. This is very difficult to do since it requires methods that properly treats wave data and selectively classifies it.

First part of this section discusses the popular method in classifying wave conditions which is the spectral analysis. The second part of this section presents the proposed technique which utilizes the Support Vector Machine.

6.1 Spectral Analysis

Spectral analysis technique utilizes the wave spectra to classify the wave conditions. The concept of wave spectra is fully discussed in Chapter 2. This technique is conventionally used by sophisticated monitoring system. To recall, if the wave data is analyzed in frequency domain, a wave is seen as a superposition of infinite number of sinusoidal wave components with different amplitudes, frequencies and phases. The decomposition of the data is done through Fast Fourier Transform (FFT). Through this, the irregularity of the waves are now expressed through wave spectrum. The sea state can be described by the characteristic parameters computed from the spectrum.

The technique starts by letting the wave sensors gather data at its predeter-

mined time. After the sampling period, FFT algorithm is applied to the wave data. It implements the Fourier transform equation with slight difference because the numeration starts at 1.

$$X_n = \frac{1}{N} \sum_{j=1}^{N} \eta_j \exp \frac{-i2\pi(j-1)(n-1)}{N} \tag{6.1}$$

where N is the length of the discrete time series. The real amplitudes, a_n can be calculated as:

$$a_n = 2\sqrt{\Re(X_n)^2 + \Im(X_n)^2} \tag{6.2}$$

The calculation of Equation 6.1 for all n-frequencies can be interpreted as the product of a matrix which is the exponential part multiplied by vector which is the surface elevation. The efficiency of FFT depends on the proper decomposition of such matrix and the permutations that reduce the number of operations needed. The possible number of decompositions depend on the length of the vector. The time it takes to execute and the required memory for FFT relies on the length or number of data points of η. FFT is fast for data which the number of points are of power of two and almost as fast for length that have only small prime factors. The smaller prime factors lead to further matrix decomposition and a fewer number of operations are required.

There are several parameters that are related with the surface elevation. These are:

mean wave height:

$$H_{mean} = \sqrt{2\pi m_0}, \tag{6.3}$$

significant wave height:

$$H_s \approx 4\sqrt{m_0}, \tag{6.4}$$

root-mean square:

$$H_{rms} = \sqrt{8m_0} \tag{6.5}$$

mean zero crossing period:

$$T_0 = \sqrt{\frac{m_0}{m_2}}, \tag{6.6}$$

mean wave period:

$$T_m = \frac{m_0}{m_1}, \tag{6.7}$$

and significant wave period:

$$\begin{aligned} T_s &= T_{peak}, && \text{for swell} \\ T_s &= 0.95T_{peak}, && \text{for wind sea} \end{aligned} \tag{6.8}$$

The advantage of the spectral analysis technique is that each of the wave components are treated individually. Since the frequencies and their corresponding amplitudes is shown through the energy density graph, the dominant frequencies can be distinguished hence the specific type of wave condition can be also be distinguished. In this study, there are three types of wave conditions are aimed to be classified which are swells, wind sea waves and mixed seas shown in Figure 6.1

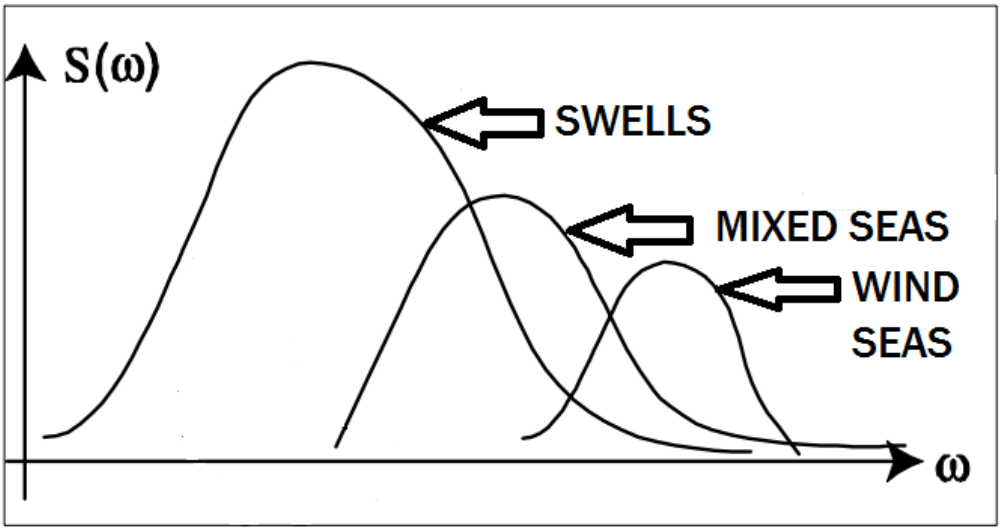

Figure 6.1: The three types of wave conditions

It is assumed that as winds blow the water surface, it will create many random waves. Since the winds are blowing in different directions, the waves tends to collide with each other making complicated patterns. These waves tend to have shorter periods. Due to the presence of wind, these waves are sometimes called wind sea waves. As the waves travel farther, the individual waves travel together,

add energy and produce more define waves. These swell waves tend to have higher energy and longer periods. Since wind systems can occur in different parts of the sea, there are tendencies that swell waves meet with new wind sea waves created by wind systems. This wave condition is called mixed sea.

These three wave conditions have specific dominant frequencies that can be identified. Figure 6.2 shows the classification of waves according to its wave period. Wind sea waves usually belong in capillary to ordinary gravity waves and swells belong in infra gravity waves to long period waves. Mixed sea belongs in the intermediate of the two wave conditions.

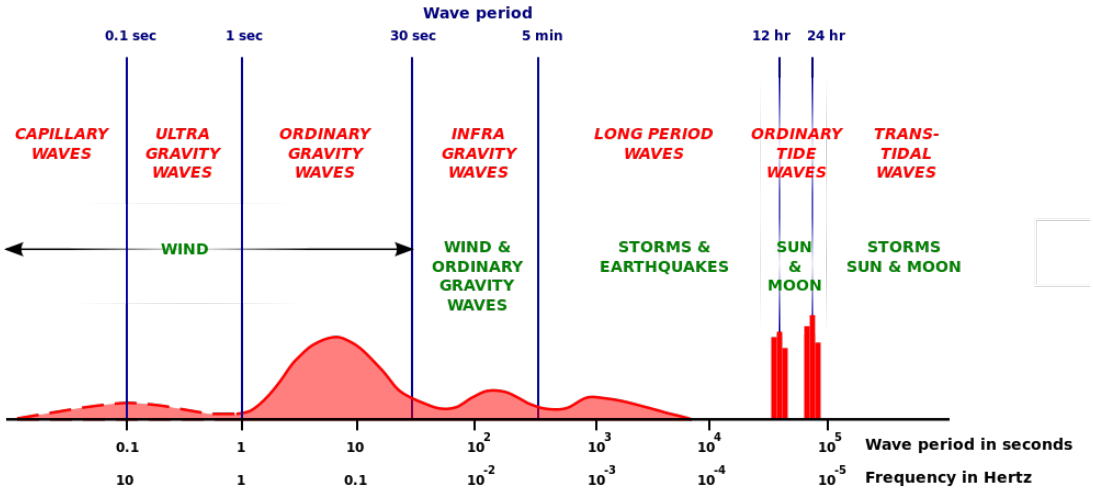

Figure 6.2: Classification of the Spectrum of Ocean Waves According to Wave Period

To demonstrate this technique, simulations of wave data using the JONSWAP spectra model are done. Table 6.1 shows the values utilized in the JONSWAP spectra model. The wind speed utilized in the simulation is fixed as $10m/s^2$. Due to this constant value, only the changes in the period and height inputs affect the generated wave data.

Figure 6.3 shows the generated wave data from the JONSWAP under the wind sea condition. Figure 6.4 shows the spectrum of the generated wave data. Figure 6.5 shows the generated wave data from the JONSWAP under the mixed sea condition. Figure 6.6 shows the spectrum of the generated wave data. Figure 6.7 shows the generated wave data from the JONSWAP under the swell wave

Table 6.1: Values Used for the Generation of Wave Data in the JONSWAP Spectra Model

	Values	
	Height (m)	Period (s)
Wind Waves	1	3.3
Mixed Sea	1.1	6
Swell Waves	2	16

condition. Figure 6.8 shows the spectrum of the generated wave data. Note that the length of all the generated wave data is about 2000 seconds. It can be observed that the all of the spectra have one distinctive peak which corresponds to the dominant frequency. The wind sea notably has lower energy as compared with the other two. This is because as mentioned previously, energy is dissipated during random collisions of waves under the presence of the wind system. The spectral width of the wind sea is noticeably wider as compared to the swell wave. This corresponds that there are many waves which have distinctive frequencies. Swell waves tend to have more defined, more peaked and higher energy wave spectra.

With the simulated wave data, the wave spectra have more distinctive peaks but this is not always the case if dealing with real wave data. The wave spectrum generated would be expected to have multiple peaks. An example of real wave data is shown in Figure 6.9. This real wave data is taken in Belmullet, Mayo County, Ireland during a storm last January 3, 2014. Figure 6.10 shows the wave spectrum generated from the real data. It can be observed that the spectrum has multiple peaks. This usually happens when the wave data is taken under a wind system. Swells that were in the area are now affected with the wind system and the energy of these waves dissipate hence, the distinctive peaks will

be lessened. Figure 6.11 shows the detailed evolution of the wave spectrum as that particular storm was experienced in the deployment location. It can be observed that the spectrum became more broadband. The energy in different frequencies also increased as the winds blow on the water surface.

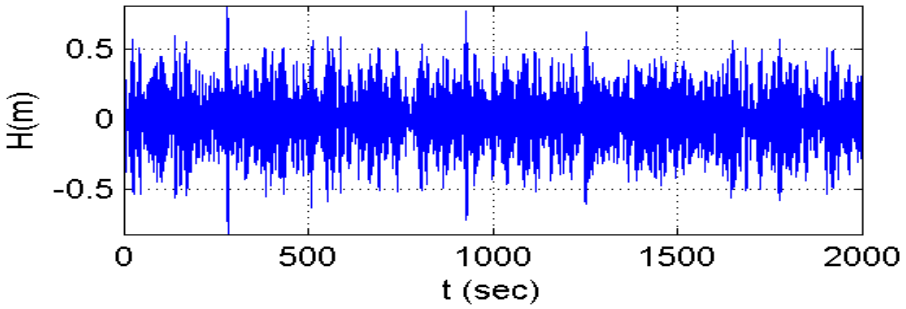

Figure 6.3: Wave Height Time Series Data of Wind Sea Condition

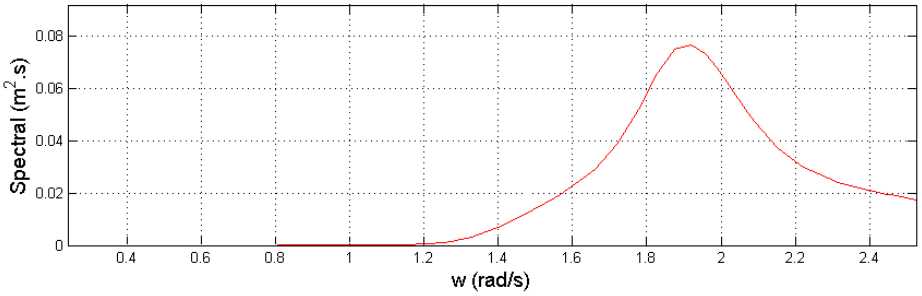

Figure 6.4: Spectrum of Wave Height Time Series Data of Wind Sea Condition

All of the data processed in this technique at this point have all been long time series data since technically the spectral analysis is a method that is usually used in sophisticated systems which has this kind of data. For the sake of exploration, spectral analysis is used to process short time series data. This is to show the capability and limitation of this conventional method.

In order to mimic the short time series data taken from the sensors, a segment of 40 seconds is taken from the each of the long wave data sets from the previous

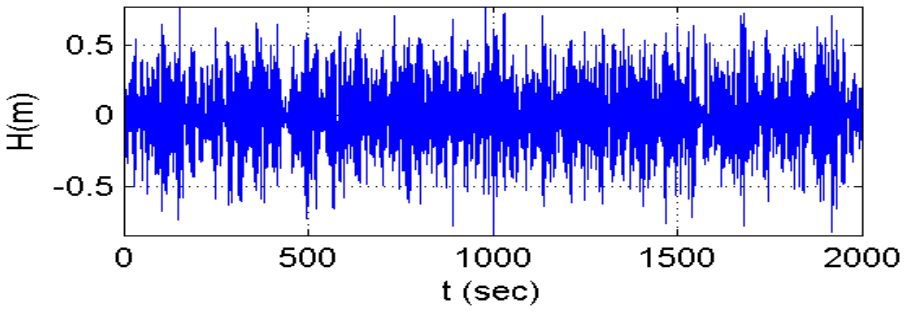

Figure 6.5: Wave Height Time Series Data of Mixed Sea Condition

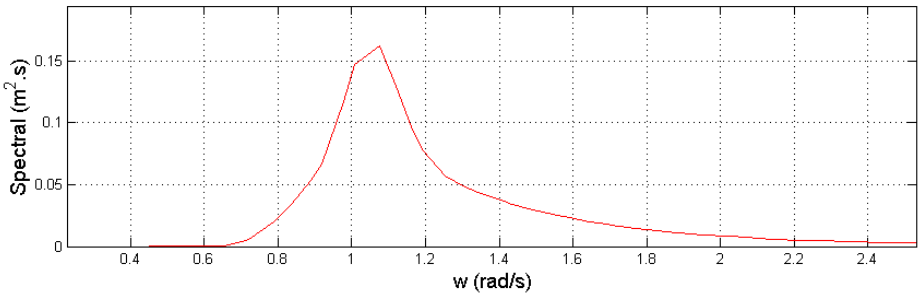

Figure 6.6: Spectrum of Wave Height Time Series Data of Mixed Sea Condition

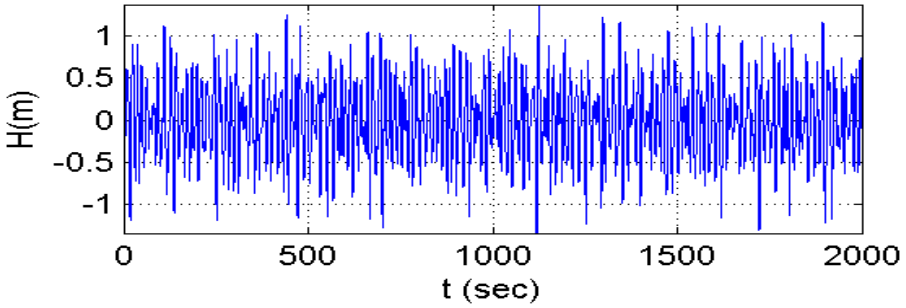

Figure 6.7: Wave Height Time Series Data of Swell Condition

simulations. Figures 6.12 to 6.17 shows the segmented data of the three wave conditions and the corresponding wave spectra. It can be seen that despite the

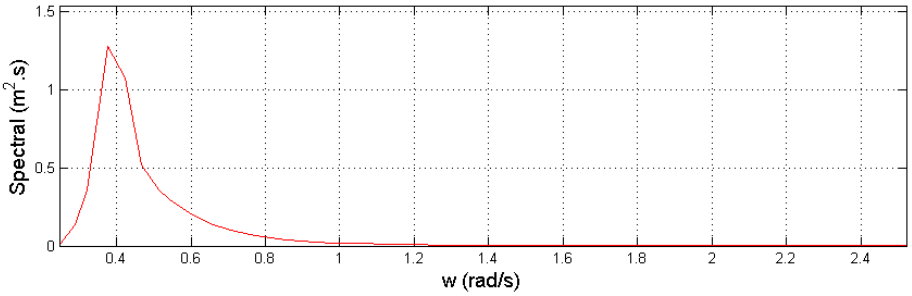

Figure 6.8: Spectrum of Wave Height Time Series Data of Swell Condition

long wave data and segmented data are from the same wave condition, the wave spectra are different. The wave spectra of the segmented data are more broadband and less peaked. This is due to the fact that the segmented data are not stationary and are prone to noise. This difference makes the chances of misclassification higher. Despite that spectral analysis is good in determining dominant wave frequencies, it is still not enough to have a good classification of wave conditions using the short time series data.

6.2 Classification of Ocean Wave Conditions through Support Vector Machines

This section is an improvement of the previous signal processing technique [59]. It is assumed previously that lower frequency waves signify swell waves and higher frequency means wind seas however, these greatly varies in different conditions. Wind seas can have long periods and swells can have shorter periods as illustrated by the classification map given by [4] shown in Figure 6.18. This is important to consider creating a classification map for our sensor data. The goal is to make a map that is fitted or adapted to short time series data. It is important to note that even though the classification map in [4] can perfectly classify the three wave conditions, the data utilized to make the map were long time series data. This

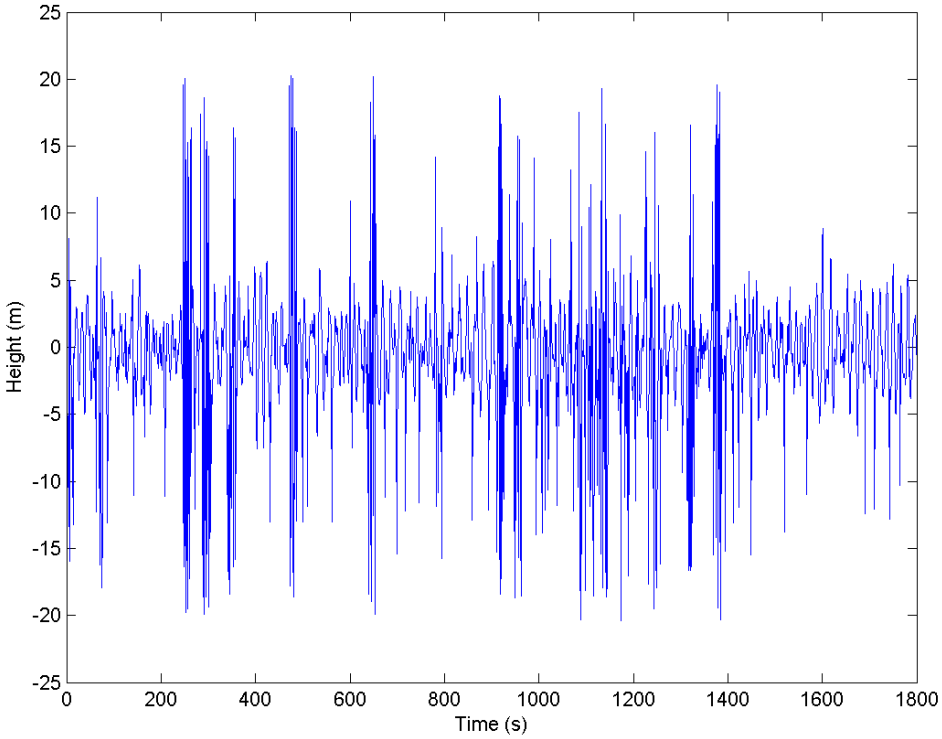

Figure 6.9: Example of a Real Wave Time Series Data

may pose a problem because the calculated parameters, significant wave height and period, from the wave spectra of the short time series data are significantly different from the long time series. The values might not be as representative to the actual classification of the wave condition.

With this in mind, an approach towards utilizing Support Vector Machines in making the classification map is explored. This technique still transforms the wave data to wave spectra however, it takes a step further by using SVM to make and train a classifier for the wave conditions.

Support Vector Machines are supervised learning algorithm that analyze data and recognize patterns for classification [60]. This algorithm corresponds to a convex optimization to determine the model parameters. The algorithm outputs an optimal hyperplane which categorizes new data. This hyperplane gives the

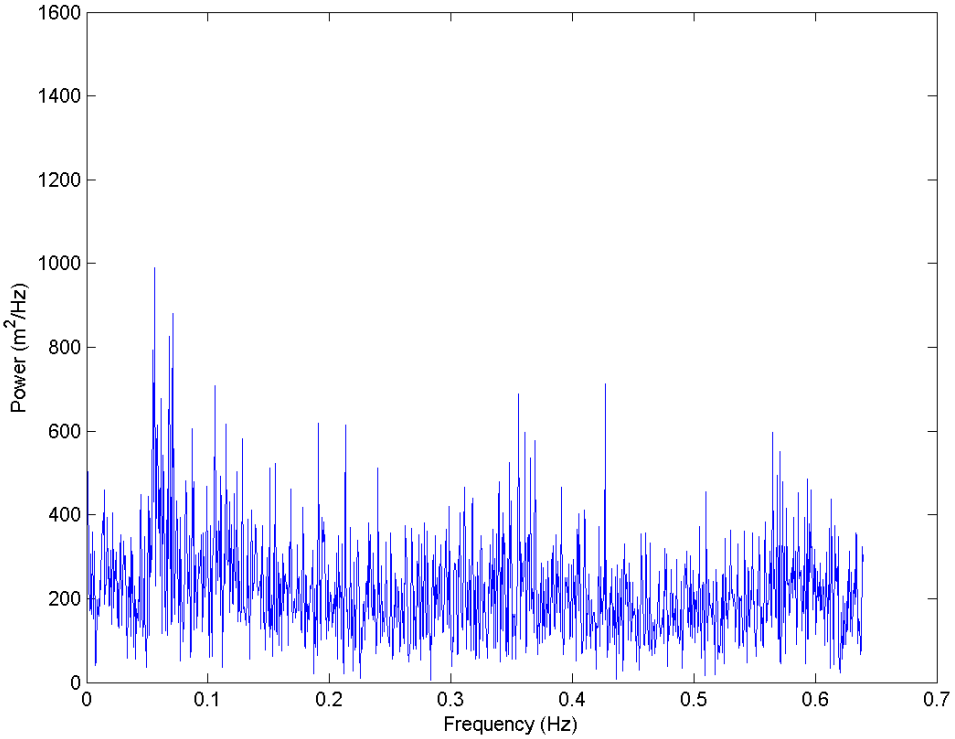

Figure 6.10: Wave Spectrum of a Real Wave Time Series Data

largest minimum distance to the training data. In this study, three classes are aimed to be distinguished from one another in the data. SVM is mainly a binary classifier however, there are some extensions of it that makes it possible to classify multiple classes.

Multiclass SVM intends to place labels to points by using the SVM where labels are drawn from finite set of elements. There are two popular methods that builds binary classifiers, one-versus-all and one-versus-one. One-versus-all distinguishes one label and the rest of the labels and the one-versus-one distinguishes every pair of the classes. In this paper, one-versus-one method is utilized.

In this method, if k is the number of classes, then $k(k-1)/2$ classifiers are constructed and each one trains data from two classes. For training data from

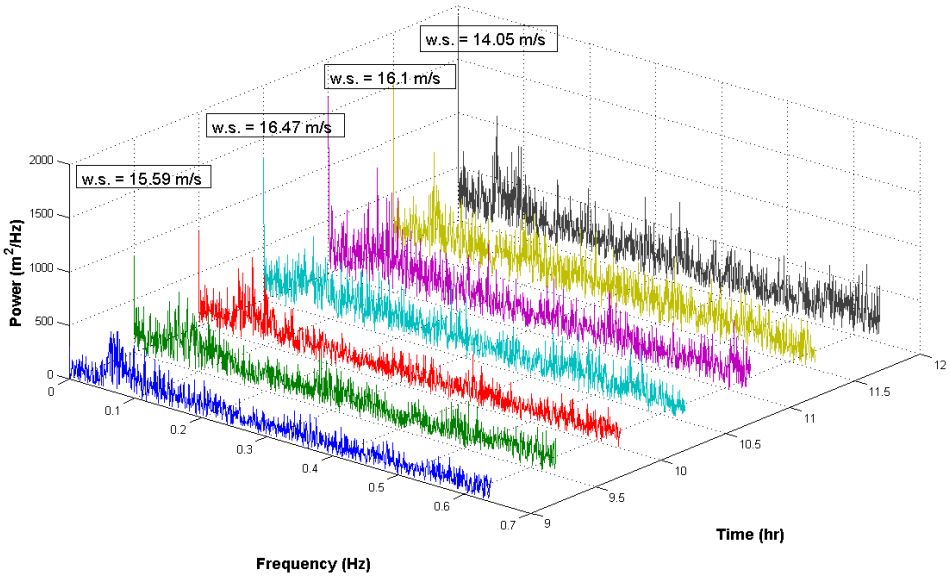

Figure 6.11: Evolution of the Waves during a Storm

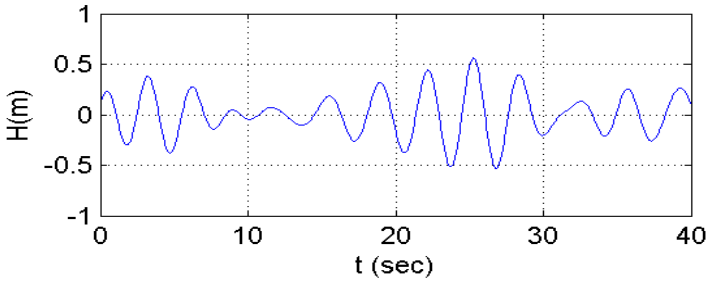

Figure 6.12: Segment from the Wind Sea Wave Height Time Series Data seen in Figure 6.3

the ith and the jth classes, the binary classification problem is solved by:

$$\begin{aligned} \min_{\mathbf{w^{ij}},\mathbf{b^{ij}},\boldsymbol{\xi}^{\mathbf{ij}}} & \frac{1}{2}(w^{ij})^T w^{ij} + C\sum_t \xi_t^{ij}(w^{ij})^T \\ & (w^{ij})^T\phi(x_t) + b^{ij} \geq 1 - \xi_t^{ij}, \text{ if } y_t = i \\ & (w^{ij})^T\phi(x_t) + b^{ij} \geq -1 + \xi_t^{ij}, \text{ if } y_t = j \\ & \xi_t^{ij} \geq 0. \end{aligned} \tag{6.9}$$

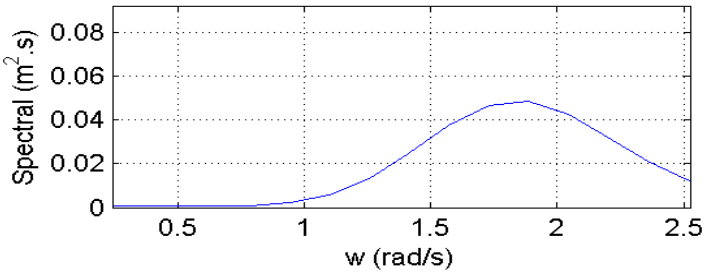

Figure 6.13: Spectrum of Segmented Data (Figure 6.12)

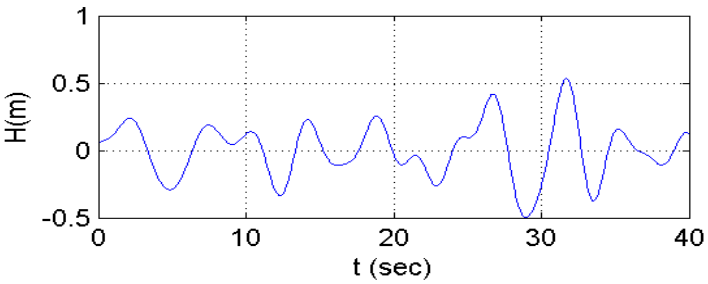

Figure 6.14: Segment from the Mixed Sea Wave Height Time Series Data seen in Figure 6.5

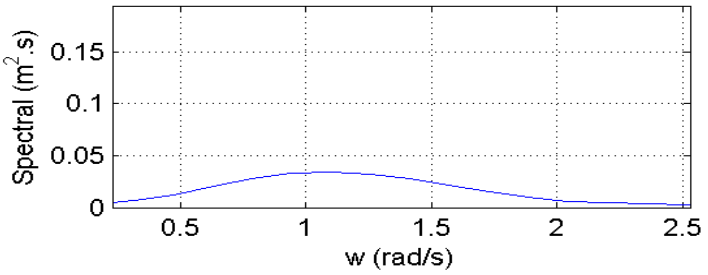

Figure 6.15: Spectrum of Segmented Data (Figure 6.14)

where x is input data, y is class, $\phi(x)$ is basis function, w is weight, C is penalty parameter, ξ is positive slack variable and b is bias parameter.

This method is a voting strategy. if $\text{sgn}((w^{ij})^T\phi(x_t) + b_{ij})$ says x is in the ith class, then the vote for ith class is added by one otherwise, jth is increased by one. x is then predicted to belong in the class with the largest vote. This voting is called "Max Wins" strategy. If the two classes have same votes, the

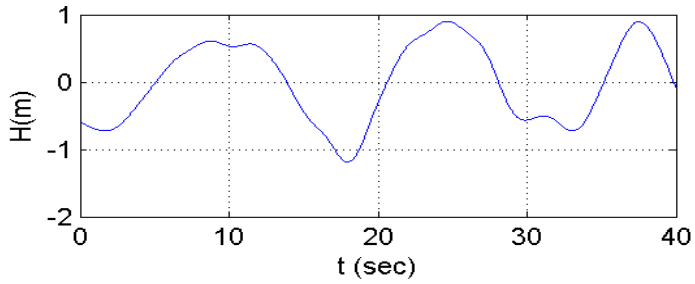

Figure 6.16: Segment from the Swell Wave Height Time Series Data seen in Figure 6.7

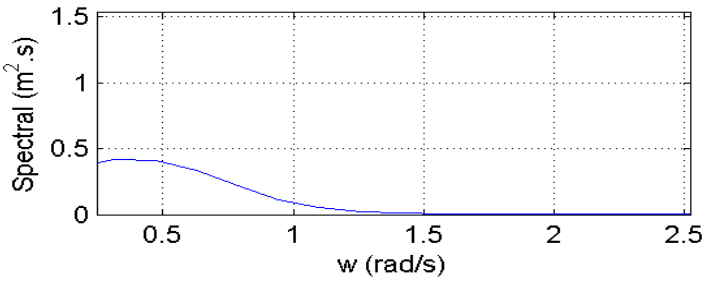

Figure 6.17: Spectrum of Segmented Data (Figure 6.16)

class appearing first in the array of storing class names will be chosen [61].

For the testing of SVM, two types of kernel functions are utilized, namely, polynomial kernel function and radial basis function. These two are suitable for training nonlinear models.

Polynomial kernels represent the similarity of vectors in feature space over polynomials of original variables. By using the degree of polynomials, it can easily create nonlinear hyperplanes.

The degree-d polynomial kernel is expressed as:

$$K(\mathbf{x}, \mathbf{y}) = (\mathbf{x}^T\mathbf{y} + c)^d \tag{6.10}$$

where x and y are vectors in input space, $c \geq 0$ is a constant which dictates the effect of higher order terms against the lower-order terms of the polynomial. As a kernel, K is the inner product in a feature space based on some mapping, ϕ.

For this study, a second degree polynomial kernel is utilized.

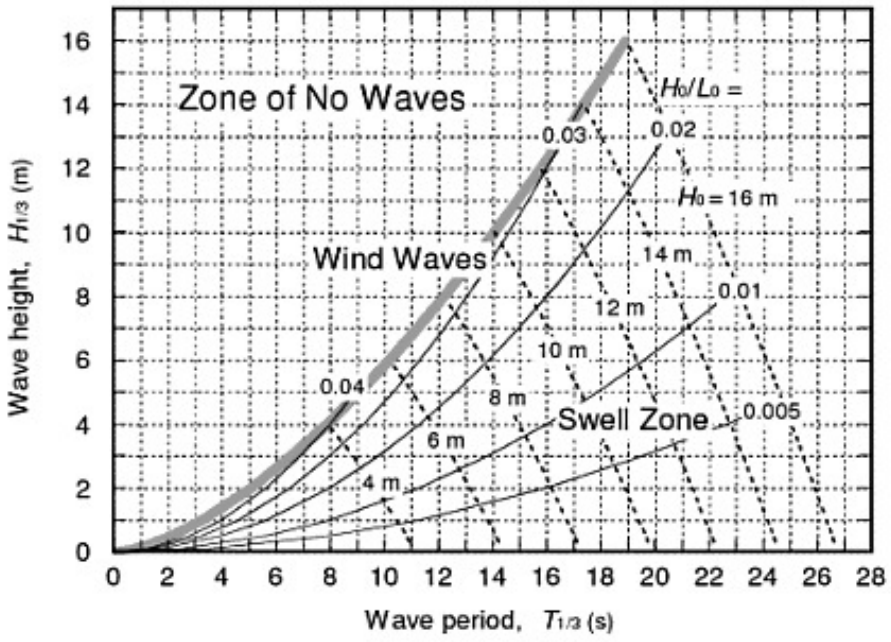

Figure 6.18: Relationship between significant wave height and period of wind sea waves and swells [4]

Radial basis function kernels are defined as:

$$K(\mathbf{x}, \mathbf{x}') = \exp(\gamma \|\mathbf{x} - \mathbf{x}'\|_2^2) \tag{6.11}$$

where $\|\mathbf{x} - \mathbf{x}'\|_2^2$ are squared Euclidean distance of two feature vectors.

The SVM algorithm follows the general steps:

1. Grid search for optimum values of hyperparameters of the chosen SVM Kernel
2. Utilize the optimum values generated in Step 1 to train the data and an SVM Model is produced
3. Use the SVM Model to predict the test data classes and calculate the accuracy of the classification

Taking the first step in the SVM algorithm, hyperparameters are identified. Setting of optimum hyperparameters for the SVM kernels is important in determining its accuracy in making the classifying models. In the polynomial kernel, its degree reflects on how flexible its decision boundary will be. For this study, a second degree polynomial is used. In radial basis function kernel, γ, adjusts the flexibility of the decision boundary while the soft margin parameter, C, controls the rigidity of the decision boundary. C penalizes margin errors. Higher values of C tend to place higher penalty resulting to a hyperplane that comes close to the several points. In order to find the optimum value of the hyperparameters, a grid search is done. The best values are then used for the training of the kernels.

The standard technique for adjusting hyperparameters is through Cross - validation (CV) technique [62]. In a K-fold cross-validation, the available data, D, is partitioned to K subsets $D_1, ..., D_K$. Each data point in D is randomly assigned to one of the subsets such that:

$$\left\lfloor \frac{|D|}{K} \right\rfloor \leq |D_i| \leq \left\lceil \frac{|D|}{K} \right\rceil . \tag{6.12}$$

Then,

$$D_{\setminus i} = \bigcup_{j=1,...,K \wedge j \neq i} D_i \tag{6.13}$$

is the union of all data points except in D_i. For each $i = 1, ..., K$, an individual model is built by applying the training data $D_{\setminus i}$. This model is evaluated by means of a cost function using the test data in D_i. The average of the K outcomes of the evaluations is called a cross-validation test performance and is used as a predictor of the algorithm when applied to D. For every split of the available data, the values of hyperparameters are used and the CV error is computed. Different combinations are tested until the lowest CV error or higher CV accuracy is achieved. This combination of the hyperparameters is then used for training the whole set D.

For this study, a 10-fold cross-validation technique is utilized to find the optimum values of C and γ. The optimum values of parameters are shown in Table 6.2. Higher CV accuracy shows that the best values for the hyperparameters do not overfit the data.

Since the optimum values of the hyperparameters are obtained, these are set

Table 6.2: Cross Validation Accuracy

	Hyperparameters	CV Acc.Rate
Polynomial Kernel d=2	C = 0.5	79.9167%
Radial Basis Function	C = 8192 γ=1.2e-04	90.5 %

to train the SVM kernels. After this training, a SVM model is produced. The model provides the number of the support vectors and its location in the feature space. As shown in Table 6.3, the total number of support vectors varies with each of the kernel.

Table 6.3: Number of Support Vectors

	# of Support Vectors
Polynomial Kernel d=2	677
Radial Basis Function	288

It can be seen that the RBF kernel requires lesser number of support vectors as compared to polynomial kernel in order to establish a better decision boundary. This signifies that the RBF kernel does not overfit the data to produce the decision boundary.

The models produced are utilized to predict the new data. Table 6.4 shows the accuracy of the classification of each of the SVM kernels. Higher accuracy signifies a better classification of the new data. After classifying the test data which are segmented data, another test is done to the classifier. 100 data points that contain ideal significant wave height-period combination are tested to the classifier. This is to test whether the classifier can classify similarly to the ideal classifier map given in Figure 6.18. Table 6.5 shows the classification accuracy of the classifier with the ideal wave data. The table shows that the accuracy for both polynomial and RBF kernels are low. The classification maps for polynomial kernel and radial basis function are shown in Figures 6.19 and 6.20. The graphs

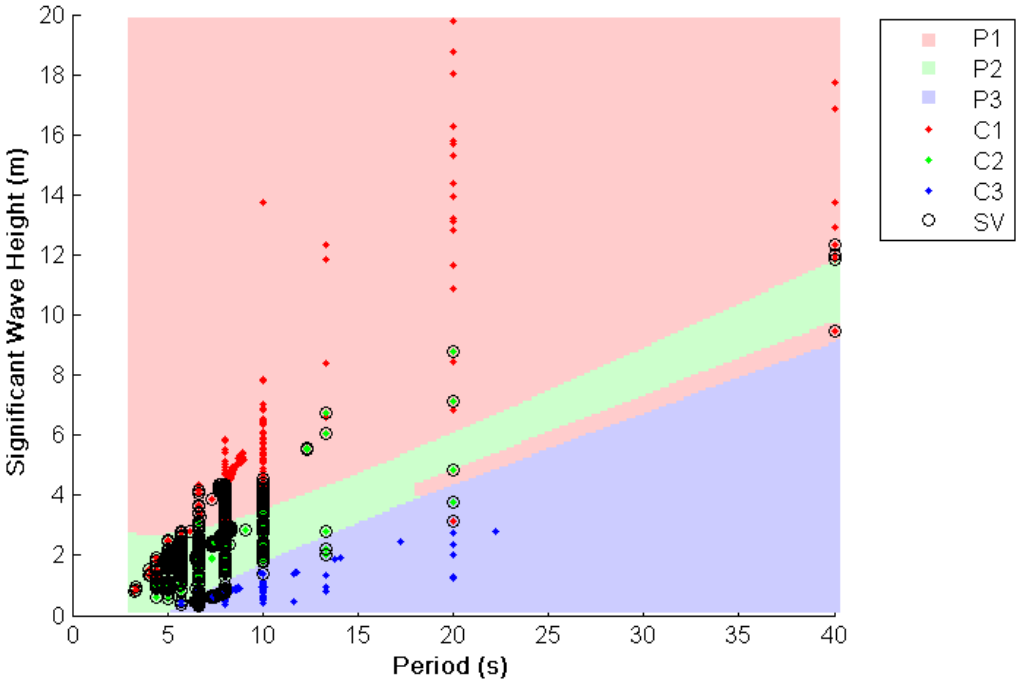

Figure 6.19: Classification map generated by polynomial kernel

show that the classifier that the experiment generated are indeed not similar to the ideal classifier map.

Table 6.4: Classification Accuracy of All Test Data

	% of Accuracy
Polynomial Kernel d=2	85.4167
Radial Basis Function	94.1667

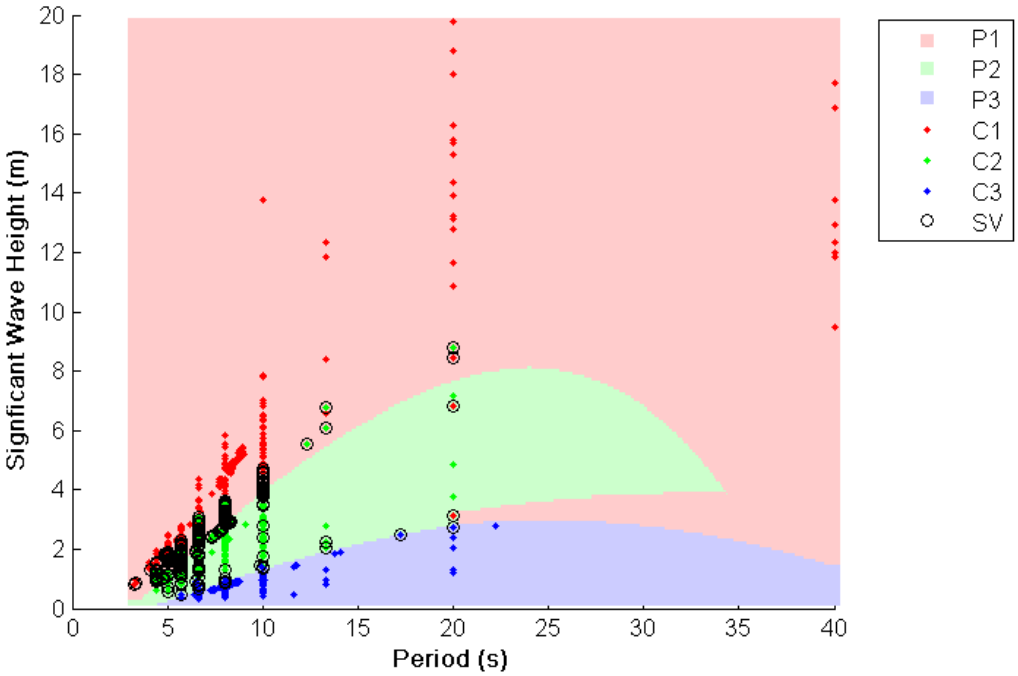

Figure 6.20: Classification map generated by RBF kernel

Table 6.5: Classification Accuracy of Ideal Wave Data

	% of Accuracy
Polynomial Kernel d=2	36%
Radial Basis Function	40%

Chapter 7

Conclusion

Ocean waves have very interesting dynamics that are difficult to monitor. These produce massive forces that destroys structures and vessels that would devastate lives and economy. Due to this, it is important to conduct ocean wave monitoring in order to deeply understand its behavior and effects. Ocean wave monitoring can be a very complex process depending on what type of methods and which areas are of interest. In this study, a local ocean wave monitoring system is considered. The process of developing a good wave monitoring system can be split into two parts: development of the hardware and formulating processing techniques that will be able to process the system data accurately and immediately.

The first part which is the development of the hardware, depends heavily on the kinds of material, devices and prototyping methods. For this study, the aim is to consider low cost and easily constructed modular devices so that the system can be readily built and deployed. It also has lower operation and maintenance costs. The system was successfully constructed meeting the goals set.

The second part which is the exploration of processing techniques to be utilized in the system, is the central focus of this study. These techniques are targeted to enable the monitoring system to (1) detect severe wave conditions, (2) process data from multiple sensors and (3) properly classify wave conditions. One major challenge in this exploration is that the system gathers short time series data to suffice the battery and memory conservation. These data range from a minute to 5 minutes worth of data. This poses a problem because the algorithms typically used in conventional monitoring systems requires long time series data. These

range to days worth of data. The standard data utilized in these algorithms range from 1024 or more data points sampled at 1 Hz. Despite the disadvantage of this kind of data, there is a merit if the processing technique is effective in handling the data. If done properly, the short time series data allows the system to produce immediate information about the current wave data. This is because the system only needs shorter duration to gather and process the data. Resorting to prediction methods which is done in conventional systems are not needed anymore. This saves the system's memory and power resources.

For the first goal of the processing technique which is the detection of severe wave conditions, there are two techniques explored. The first technique is the threshold technique which utilizes fixed threshold levels in determining the wave conditions. The threshold levels are chosen from the response of the sensors using the double pendulum test platform. The double pendulum test platform was constructed because it is difficult to gather data from severe wave conditions. This method is a straightforward approach since it counts the instantaneous values which exceed the set threshold value. The count values are then evaluated as to how severe the wave conditions are. The higher count signifies severe wave conditions. The sensitivity of the wave sensors are dependent on the threshold levels. The threshold levels can be adjusted depending on how sensitive the user wants their wave sensors to be. This is simple and effective but this is not sufficient because the threshold levels are too rigid and the values are taken from a test platform. It might not be as effective if it will be utilized using the real wave data. The second technique explored is the statistical analysis technique. This answers the problems encountered in the threshold technique which is the rigidity of the threshold levels. The wave sensors are first deployed to the target areas and gather data on a fine weather condition. These data are then considered as baseline data. The statistical parameters - kurtosis and skewness are generated from the gathered data. These kurtosis and skewness values are considered as the values for the normal wave condition in the particular area. Kurtosis and skewness values of the newly gathered wave data will then be compared to these normal values. Large difference values from the normal values signify severe wave condition. This technique avoids the tedious comparison between instantaneous data by processing the data by segments. It considers the data gathered within

the sampling duration as a data segment. The two techniques enables the system to detect severe wave conditions through comparison to the normal conditions. The statistical analysis technique is a better method since it employs a better comparative data which are location dependent and it processes data every after sampling duration which minimizes the usage of the system's resources.

For the second goal of the processing technique which is to process data from multiple sensors, a technique that processes nonlinear multivariate data is explored. This technique is the independent component analysis (ICA). Given that there are multiple sensors in the network, the gathered data can be used to approximate the source signals or the dominant waves that are in the area. There are no a priori information about these waves and the mixing process hence it is difficult to retrieve these source signals without resorting to blind signal deconvolution (BSD). ICA works well in BSD. The concept is that the data from the sensors are considered as the observed signals and a demixer is produced to inversely recover the source signals. In this technique, there are several methods in setting up the demixer and the treatment of the approximations. There are four methods tested - FIR approximation by Zhang et al. [2] , IIR method by Tanaka et al. [3], first improved method by the author et al. [56] and the further improved method by the author et al. [57]. It can be seen in the results shown in Figures 5.13 and 5.20 that the first and second improved method have faster convergence compared to the other two methods. This is because these methods have more direct and explicit treatment to its cost function. The methods also have lower RMSE as compared to the other two methods. Despite that ICA works best in signal recovery, there are issues with it on its assumptions for its input signals. They have to be spatially and temporally i.i.d. and at most have one Gaussian distribution. These conditions are hard to suffice with real wave data. Also, the recovered and approximated source signals may not correctly represent the actual source waves because ICA has ambiguities such as the variance, order and frequency ambiguities. Unfortunately, these three parameters - variance, order and frequency values are very important in dealing with ocean wave data hence, utilizing ICA may not be so practical. Note that for the simulations and testing of ICA in this study, a synthetic M-pseudorandom binary signal are utilized instead of actual ocean data.

For the third goal which is to classify the wave conditions, two techniques are explored. The first technique is the spectral analysis. This is considered as the conventional method utilized in sophisticated systems. This method requires long time series data. This method firstly transforms the wave data from the time domain to the frequency domain to prepare it for analysis. When considering raw time series data, it is difficult to comprehend the dynamics since the wave components are superimposed with each other. The wave record appears to have a rather noisy or complicated pattern. This is remedied if the wave record is transformed in the frequency domain. Through this transformation, the dominant wave frequency in the wave data can be distinguished. Identifying dominant wave frequencies directly determines the wave conditions. There are three wave conditions targeted to be identified in this study. These are wind seas, swell waves, and mixed seas. Wind seas indicate that there is a current wind system in the area of interest. Constant pounding of the wind and clashing of waves create shorter period waves. Swell waves indicate that there are no wind systems in the area of interest. Since the area has no interferences from major wind system, the waves tend to have longer periods and more defined higher energy. Mixed seas indicate that there is a wind system in the nearby area. The waves in this category tend to have a mix of short and long periods. Since this method can identify the dominant wave frequency, it is effective in distinguishing these three conditions. Having a defined dominant wave frequency requires long time series data hence this method is utilized in sophisticated systems. Since this method has this requirement, it cannot be utilized in short time series data and this is shown in Figures 6.12 to 6.17. Also, despite that it can effectively classify wave conditions, there are some cases where it might fail since there are times that these wave conditions have different frequencies as expected. This is shown in the map provided by [4] shown in Figure 6.18. Also, wave spectra of real ocean waves have multiple peaks hence there are multiple dominant frequencies. Note that for the testing and evaluation of this technique, a simulator is used to generate wave data. The second technique explored for the classification of wave conditions is the Support Vector Machine. Wave conditions can be identified and mapped according to their significant wave height and period similar to the map in [4]. This is practical since wave conditions are difficult to identify. It would be

natural to utilize the map in [4] however, this map is for long time series data. Using this may incorrectly identify wave conditions. Thus, this motivated this study to make a map or a classifier model trained by SVM. In order to make this map, the wave simulator from the previous technique is utilized to generate several data. The simulator generated long time series data from different wave conditions and from that, data segments are taken to mimic the short time series data. The significant wave height and period are calculated and the data segment is labelled according to which wave condition it was taken from. Various data segments are processed and train data and test data are created. These data are then used to produce a classifying model through SVM training. There are two SVM kernels tested in this technique - polynomial and radial basis function. It can be seen in the results that the SVM radial basis function kernel produced a better classifying map. This efficiently classified the short time series data. This technique sufficiently and effectively produced a classification map for short time series data. By having this classification map, immediate identification of wave condition can be easily done.

Given the results provided by the techniques, the three goals for the wave monitoring system are achieved. These processing techniques overcame the challenge of dealing with short time series data. By programming these techniques to the system, they will enable the local ocean wave monitoring system to function in similar and even in an improved way as the sophisticated monitoring systems.

Chapter 8

Discussion and Future Work

8.1 Recommendation

Despite the thorough testing and evaluation of the processing techniques, only the threshold technique and the statistical analysis technique are the ones tested on the actual wave data gathered from the local ocean wave monitoring system. This is largely because the field deployments were limited hence data are limited. For the ICA method, it is suggested that in order for it to be fully utilized, preprocessing of wave data (i.e. data transformations) should be done. Methods to address the ambiguities of ICA is recommended to be explored. For the SVM method, it is recommended to explore other kernel functions. Other kernel methods may provide a better classification map.

8.2 Future Work

Since this study is exploratory, there are several future works considered for this study. First is for further field deployments of the local ocean wave monitoring system. Through these deployments, several data can be acquired. These data can be utilized by the processing techniques for further evaluation. Next future work is to explore on other algorithms (i.e. wavelet theory) that are effective in detecting anomalies such as rouge or extreme waves. Another one is to test other processing algorithms that might be able to process data from multiple sensor.

ICA has encountered a lot of challenges in study hence, it is better to find other algorithms that might be less complicated as ICA. Another is to explore SVM kernels for training the classification map. These kernels might provide a better classification map for short time series data.

Acknowledgements

"The fishermen know that the sea is dangerous and the storm terrible, but they have never found these dangers sufficient reason for remaining ashore" - Vincent Van Gogh

First and foremost, I offer this humble work to God Almighty who has provided me life, passion, knowledge, courage and perseverance to pursue this great undertaking. *Ad Majorem Dei Gloriam!*

Next, I would like to extend my deepest gratitude to my supervisor, Professor Kenji Sugimoto. I am forever thankful to him for giving me this opportunity to achieve my dream. His support, guidance and encouragement made this study possible. *My sincerest thank you, Sensei!*

I would like to thank Assistant Professor Takamitsu Matsubara for his valuable lessons and advices both in academic and general life. Even for a short period of guidance, he has enlightened me about the bittersweet process of obtaining a doctorate degree and what can i do after I have obtained. *Keep inspiring young brilliant minds, Sensei!*

I would like to thank Professor Kentaro Hirata for his guidance and advices. He has inspired me to challenge myself. *Thank you, Sensei!*

I would like to extend my gratitude to my thesis committee, Professor Kenji Sugimoto, Professor Minoru Okada, Visiting Professor Kentaro Hirata and Assistant Professor Takamitsu Matsubara for their helpful and constructive comments for this dissertation.

I also want to express my deep gratitude to Professor Gregory Tangonan. He has always been my inspiration in pursuing research despite all of the challenges ahead. He is my mentor and idol in the field of research and business. *I am*

forever indebted, Sir Greg!

I would also like to thank all the members of the Intelligent System Control Laboratory. They have welcomed me and accompanied me in this journey. *Let the dream and passion live on!*

I would like to thank the administration of Nara Institute of Science and Technology for choosing and granting me the NAIST International Scholarship. Through this prestigious scholarship, I am able to pursue my dream and my parents's dream for me.

I would like to also thank the Filipino community in NAIST for their valuable support. They have been with me through the turmoils and jovialities.

I want to thank Ms. Erlyn Manguilimotan, Ms. Louie Jane Zamora, Dr. Gemalyn Abrajano and Dr. Inga Inhulsen for their company. *Life wouldn't be as happy without the Ich Liebe Dich girls!*

I would like to thank my bestfriend, Mr. Marc Ericson Santos. He has been there for me always. Having him as my bestfriend gave me strength and tenacity to achieve my goals. *Thank you very much, Marcky!*

I would like to thank Ms. Gerardine Basanez who has been my cheerleader even though we are thousand miles apart. *Thank you, Gerardine!*

I also would like to thank my close friend, Mr. David Joseph Tan. His encouraging words always kept me in track of my goals. Despite all of my whims, he has endured to listen each of it. *Thank you for being my shock-absorber, David!*

I would like to express my innermost gratitude to my solace, Michael Leo O'Rourke. He has supported and challenged me to become a better person. *Thank you for being the serenity in my troubled seas. I will always be thankful to God for you.*

Finally, I would like to dedicate this dissertation to my parents, Ismael Marimon and Meriam Marimon. They have nurtured, molded and encouraged me to blossom to my true potential. *Thank you for showing me the most genuine love possible here on earth. I am forever your daughter. To Mama, though you are not here anymore in this world, I still feel your presence and love and they surround me everyday. To Papa, you will always be my rock and my epitome of strength. I love you my dearest Mama and Papa!*

To everyone who has become a part of my journey, I sincerely thank you all.

Publication List

Journal

1. Maricris C. Marimon, Gregory L. Tangonan, Nathaniel Joseph C. Libatique, and Kenji Sugimoto. In *Development and Evaluation of Wave Sensor Nodes for Ocean Wave Monitoring*, IEEE Systems Journal, DOI 10.1109 / JSYST.2013.2284102 (to appear). [Corresponds to Chapter 3]

International Conferences

1. Maricris C. Marimon, Takamitsu Matsubara, Kenji Sugimoto, In *Classification of Ocean Wave Condition Using Support Vector Machine*, 33rd Chinese Control Conference CCC2014, to appear, Nanjing, China (2014) [Corresponds to Chapter 4]

2. Maricris C. Marimon, Daisuke Tanaka, Kenji Sugimoto, In *A Scheme for Independent Component Analysis via Adjoint Polynomial Matrix*, The 45th ISCIE International Symposium on Stochastic Systems Theory and Its Applications, Okinawa, Japan (2013) [Corresponds to Chapter 4]

3. Maricris C. Marimon, Daisuke Tanaka, and Kenji Sugimoto, In *Improved Blind Deconvolution Scheme for System Identification*, The SICE Annual Conference 2013 SICE 2013, Nagoya, Japan (2013) [Corresponds to Chapter 4]

4. Maricris C. Marimon and Kenji Sugimoto, In *Threshold Design for Low Cost Wave Sensors Through Statistical Analysis of Data*, 7th International

Conference on System of Systems Engineering IEEE SOSE 2012, Genova, Italy (2012) [Corresponds to Chapter 4]

Domestic Conferences

1. Maricris C. Marimon, Daisuke Tanaka, Kenji Sugimoto, In *Adjoint Polynomial Matrix Approach to Independent Component Analysis and Semi-blind Identification*, 56th Joint Automatic Control Conference, Niigata, Japan (2013) [Corresponds to Chapter 4]

2. Maricris C. Marimon and Kenji Sugimoto, In *Designing Threshold Criteria for Low Cost Wave Sensors using Statistical Data Analysis*, 55th Joint Automatic Control Conference, pp. 669-672, Kyoto, Japan (2012) [Corresponds to Chapter 4]

Bibliography

[1] *Guide to Wave Analysis and Forecasting*. WMO No. 702. World Meteorological Organization, Geneva, Switzerland, 1998.

[2] L. Zhang et al. Blind deconvolution of dynamical systems: A state-space approach. *Signal Processing*, 4(2):113–130, 2000.

[3] D. Tanaka et al. Blind identification of polynomial matrix fraction for disturbance rejection. In *7th IFAC Symposium on Robust Control Design (ROCOND'12)*, pages 69–74, Aalborg, Denmark, 2012.

[4] Y. Goda. *Random Seas and Design of Maritime Structures*, volume 33 of *Advance Series on Ocean Engineering*. World Scientific Publishing Co. Pte. Ltd., third edition, 2010.

[5] M. Marimon et al. Development and evaluation of wave sensor nodes for ocean wave monitoring. *IEEE Systems Journal*, (DOI 10.1109/JSYST.2013.2284102).

[6] M. Marin et al. Wave monitoring with wireless sensor networks. In *4th International Conference on Intelligent Sensors, Sensor Networks and Information Processing*, Sydney, Australia, 2008.

[7] F. de Pascalis et al. Climate change response of the mar menor coastal lagoon (spain) using a hydrodynamic finite element model. *Estuarine, Coastal and Shelf Science*, 114:118–129, 2012.

[8] J. W. Miles. On the generation of surface waves by shear flows. *Fluid Mechanics*, 3(2):185–204, 1957.

[9] *Extreme Ocean Waves*. Springer, London, 2008.

[10] V. Kudryavtsev et al. Modulation of wind ripples by long surface waves via the air flow - a feedback mechanism. *Boundary - Layer Meteorology*, 83(1):99–116, April 1997.

[11] Longuet-Higgins. M. S. On the statistical distribution of heights of sea waves. *Journal of Marine Research*, 11:245–266, 1952.

[12] J. R. Halliday et al. The application of short term deterministic wave prediction to offshore electricity generation. In *International Conference on Renewable Energies and Power Quality*, Zaragosa, Spain, 2005.

[13] A. E. Gent. What does the "multi" in multi-mission mean? evolution of the t-ags 60 class oceanographic survey ships. In *Proceedings of the IEEE Conference OCEANS*, volume 2, pages 949–955, Rhode Island, USA, 2000.

[14] C. A. Balfour et al. The use of ships of opportunity for irish sea based oceanographic measurements. In *Proceedings of the IEEE Conference OCEANS*, pages 1–6, Vancouver, Canada, 2007.

[15] C. R. Barnes et al. The neptune project - a cabled ocean observatory in the ne pacific: Overview, challenges and scientific objectives for the installation and operation of stage 1 in canadian waters. In *Proceedings of the Underwater Technology and Workshop on Scientific Use of Submarine Cables and Related Technologies*, pages 308–313, Tokyo, Japan, 2007.

[16] U. M. Cella et al. Wireless sensor networks in coastal marine environments: A study case outcome. In *Proceedings of the 5th International Workshop on Underwater Networks*, pages 1–8, California, USA, 2009.

[17] L. Emery et al. Autonomous collection of river parameters using drifting buoys. In *Proceedings of the IEEE Conference OCEANS*, pages 1–7, Washington, USA, 2010.

[18] A. Kwok et al. Deployment of drifters in a piecewise-constant flow environment. In *Proceedings of the 49th IEEE Conference on Decision and Control (CDC)*, pages 6584–6589, Georgia, USA, 2010.

[19] J. K. Choi et al. Safe operation of an autonomous underwater towed vehicle: Towed force monitoring and control. In *Automation in Construction*, volume 20, pages 1012–1019, 2011.

[20] J. H. J. Leach. The development of a towed vehicle for optical mapping in shallow water. In *Proceedings of the IEEE Conference OCEANS*, volume 3, pages 1455–1458, Nice, France, 1998.

[21] C. Kaminsky. 12 days under ice - an historic auv deployment in the canadian high arctic. In *Proceedings of the 2010 IEEE/OES Autonomous Underwater Vehicles (AUV)*, number doi:10.1109/AUV.2010.5779651, California, USA, 2010.

[22] I. Masmitja et al. Development of a control system for an autonomous underwater vehicle. In *Proceedings of the 2010 IEEE/OES Autonomous Underwater Vehicles (AUV)*, number doi:10.1109/AUV.2010.5779647, California, USA, 2010.

[23] G. Meinecke et al. Hybrid - rov - development of a new underwater vehicle for high-risk areas. In *Proceedings of the IEEE Conference OCEANS*, pages 1–7, Hawaii, USA, 2011.

[24] K. Kawaguchi et al. Subsea engineering rov and seafloor observatory construction. In *Proceedings of the 2011 IEEE Symposium on and Workshop on Scientific Use of Submarine Cables and Related Technologies (SSC), Underwater Technology (UT)*, pages 1–6, Tokyo, Japan, 2011.

[25] B. G. Ferguson et al. Sensing the underwater acoustic environment with a single hydrophone onboard on undersea glider. In *Proceedings of the IEEE Conference OCEANS*, pages 1–5, Washington, USA, 2010.

[26] I. F. Akyildiz et al. Underwater acoustic sensor networks: Research challenges. *Adhoc Networks*, 3:257–279, 2005.

[27] I. F. Akyildiz et al. Wireless sensor networks: A survey. *Computer Network*, 38:393–422, 2002.

[28] T. Pedersen et al. Directional wave measurements from a subsurface buoy with an acoustic wave and current profiler. In *OCEANS 2007 Proceedings*, Vancouver, Canada, 2007.

[29] A. V. Babanin et al. Measurement of wind waves by means of a buoy accelerometer wave gauge. *Physical Oceanography*, 4(5):399–407, 1993.

[30] L. C. Bender et al. A comparison of methods for determining significant wave heights applied to a 3-m discus buoy during hurricane katrina. *Atmospheric and Oceanic Technology*, 27:1012–1028, 2010.

[31] J. Font et al. Smos: The challenging sea surface salinity measurement from space. 98:649–665, 2010.

[32] D. Prandle. Operational oceanography - a view ahead. *Coastal Engineering*, 41:353–359, 2000.

[33] C. Albaladejo. A low-cost sensor buoy system for monitoring shallow marine environments. *Sensors*, 12(7):9613–9634, 2012.

[34] C. Albaladejo et al. Wireless sensor networks for oceanographic monitoring: A systematic review. *Sensors*, 7:6948–6968, 2010.

[35] B. Benson et al. Real time telemetry options for ocean observing systems. In *European Telemetry Conference*, Munich, Germany, 2008.

[36] P. Jiang et al. Design of a water environment monitoring system based on wireless sensor networks. *Sensors*, 9:6411–6434, 2009.

[37] X. Yang. Design of a wireless sensor network for long-term, in-situ monitoring of an aqueous environment. *Sensors*, 2:455–472, 2002.

[38] C. Buratti. An overview on wireless sensor networks technology and evolution. *Sensors*, 9:6869–6896, 2009.

[39] D. Hugo et al. Low-cost marine monitoring: From sensors to information delivery. In *Proceedings of the IEEE Conference OCEANS*, pages 1–7, Hawaii, USA, 2011.

[40] A. Sieber et al. Low power wireless buoy platform for environmental monitoring. 64:25–42, 2010.

[41] F. M. White et al. *Fluid Mechanics*. Mcgraw-Hill, New York, USA, 1998.

[42] T. Soukissian et al. Poseidon: A marine environmental monitoring, forecasting and information system for the greek seas. *Mediterranean Marine Science*, 1(1):71–78, 2000.

[43] T. Soukissian et al. An integrated wave monitoring network for the hellenic seas. In *27th International Conference on Offshore Mechanics and Arctic Engineering ASME 2008*, Estoril, Portugal, 2008.

[44] J. Kuperus. Wave monitoring using wireless sensor nodes. M.eng. thesis, University of Melbourne, Melbourne, Australia, 2009.

[45] M. Marimon et al. Low cost sensor system for wave monitoring. In *7th International Conference on Intelligent Sensors, Sensor Networks and Information Processing*, Adelaide, Australia, 2011.

[46] F. Tanveer et al. Design and development of a sensor fusion based low cost attitude estimator. *Space Technology*, 1(1), 2011.

[47] Starlino. A guide to using imu in embedded applications, 2009.

[48] K. Vogt. Hamiltonian chaos: The double pendulum; simulations, poincare plot and sonification. *SE Computeroientierte Physik*, 2006.

[49] R. Nelson. The pendulum - rich physics from a simple system. *American Journal of Physics*, 54(2), February 1986.

[50] M. Marimon et al. Threshold design for low cost wave sensors through statistical analysis of data. In *7th International Conference on System of Systems Engineering*, Genoa, Italy, 2012.

[51] M. Marimon et al. Designing threshold criteria for low cost wave sensors using statistical data analysis. In *55th Joint Automatic Control Conference*, pages 669–672, Kyoto, Japan, 2012.

[52] L. White et al. An automatic sea state calculator. In *OCEANS 2000 MTS/IEEE Conference Proceedings*, volume 3, 2000.

[53] R. Norland et al. A comparison of sea waves on open sea and coastal waters. In *2001 CIE International Conference on Radar Processing*, pages 423–426, 2001.

[54] *Independent Component Analysis*. John Wiley and Sons, Inc, 2001.

[55] A. Cichocki et al. *Adaptive Blind Signal and Image Processing, Learning Algorithms and Applications*. John Wiley and Sons, Inc, 2002.

[56] M. Marimon et al. Improved blind deconvolution scheme for system identification. In *The SICE Annual Conference 2013 (SICE2013)*, Nagoya, Japan, 2013.

[57] M. Marimon et al. Adjoint polynomial matrix approach to independent component analysis and semi-blind identification. In *56th Joint Automatic Control Conference*, Niigata, Japan, 2013.

[58] M. Marimon et al. A scheme for independent component analysis via adjoint polynomial matrix. In *45th ISCIE International Symposium on Stochastic Systems Theory and Its Applications*, Okinawa, Japan, 2013.

[59] M. Marimon et al. Classification of wave condition using support vector machine. In *33rd Chinese Control Conference (CCC2014)*, page to appear, Nanjing, China, 2014.

[60] C. Bishop. *Pattern Recognition and Machine Learning*. Verlag New York, Inc., New Jersey, USA, 2006.

[61] C. W. Hsu et al. A comparison of methods for multi-class support vector machines. *IEEE Transactions on Neural Networks*, 13(2):415–425, 2002.

[62] T. Hastie et al. *The Elements of Statistical Learning*. Springer - Verlag, 2008.